

A Study of Hypertensive Retinopathy Changes for Stroke Prediction

by

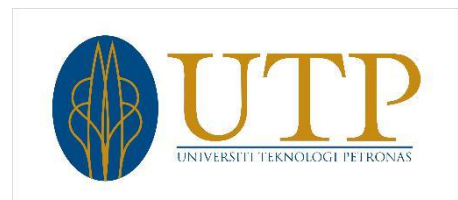
Ng Guan Shen

18440

Dissertation submitted in partial fulfilment of
the requirements for the
Bachelor of Engineering (Hons)
(Electrical and Electronic)

JANUARY 2017

Universiti Teknologi PETRONAS
Bandar Seri Iskandar
31750 Tronoh
Perak Darul Ridzuan



CERTIFICATION OF APPROVAL

A Study of Hypertensive Retinopathy Changes for Stroke Prediction

by

Ng Guan Shen

18440

A project dissertation submitted to the
Electrical and Electronic Programme
Universiti Teknologi PETRONAS
in partial fulfilment of the requirement for the
BACHELOR OF ENGINEERING (Hons)
(ELECTRICAL AND ELECTRONIC)

Approved by,

(Dr. Lila Iznita Izhar)

UNIVERSITI TEKNOLOGI PETRONAS

TRONOH, PERAK

January 2017

CERTIFICATION OF ORIGINALITY

This is to certify that I am responsible for the work submitted in this project, that the original work is my own except as specified in the references and acknowledgments, and the original work contained herein have not been undertaken or done by unspecified sources or persons.

NG GUAN SHEN

ABSTRACT

Hypertensive retinopathy is an ailment that is highly connected to hypertension which help in stroke prediction. The presence of hypertensive retinopathy is diagnosed through image processing on the fundus image to identify the possible microvascular retinal abnormalities signs that lead to hypertension. Arterio-Venous Ratio (AVR) value is one of the main indicator of hypertensive retinopathy, useful for grading severity of hypertensive retinopathy and for prediction of risk of stroke. Image preprocessing were performed in this work to extract vessels in fundus image. In this thesis, fundus images were acquired from VICAVR and DRIVE databases.

ACKNOWLEDGEMENT

First and foremost, I would like to take this opportunity to extend my heartfelt gratitude to my Final Year Project (FYP) supervisor, Dr. Lila. I am grateful for her dedicated supervision and support in facilitating me in completing this research. All the hurdles and deterrents encountered during the research would not be easily and successfully overcome without her help. Her great insights and experience had made the completion of this research smoother and easier. Special thanks to Dr. Cheng-Kai Lu for his help in guiding and validating the work.

Besides that, I would like to express my sincerest thanks to all the FYP committees for their efforts and patience in providing necessary guidance i.e. guidelines in writing paper which ease the paper creation and submission, time allocation for viva and so on. Not to forget, thank you to Universiti Teknologi Petronas Electrical & Electronic Engineering faculty for bestowing the research opportunity and necessary funds to all the final year students so that we could be more competitive and innovative.

Furthermore, I would like to express my deepest gratitude and thankfulness to my family for their unabated loves, spiritual and financial supports which compelled me to do my best in completing this research. When I am feeling demotivated, their advices and supports were the drives that kept me motivated and striving for the best. In addition, I would love to sincerely thank and acknowledge my peers for their helps as well as advices in making this research more exhilarating and interesting.

Last but not least, I would like to extend my gratitude to all the parties that had helped and contributed directly or indirectly to the success of this research. Special thanks to VICAVR, DRIVE for publicly available fundus image databases. This research would not be successful without all the helps given. All the loves, advices, moral supports, and funds given to me was what motivated me to continue the research despite numerous setbacks encountered. Once again, I am truly thankful for all the helps and supports given throughout the research duration.

TABLE OF CONTENTS

CERTIFICATION OF ORIGINALITY	i
ABSTRACT	ii
ACKNOWLEDGEMENT	iii
LIST OF FIGURES	vi
LIST OF TABLES	vii
CHAPTER 1: INTRODUCTION	1
1.1	Background of Study	1
1.2	Problems Statements	2
1.3	Objectives & Scope of Study	3
CHAPTER 2: LITERATURE REVIEW	4
2.1	Related Work	4
2.1.1	Relationship between Retinal Signs and Stroke	4
2.1.2	Hypertensive Retinopathy and Arterio-Venous Ratio (AVR)	5
2.2	Critical Analysis	8
CHAPTER 3: METHODOLOGY	9
3.1	Process Methodology	9
3.2	Gantt Chart & Key Milestones	10
3.3	Approach Overview	12
3.3.1	Preprocessing of Fundus Image	13
3.3.2	Extraction of Blood Vessels	16
CHAPTER 4: RESULTS AND DISCUSSIONS	19
4.1	Extracted Vessel	19
4.2	Discussion on Standard Artery and Vein Classification	23
4.3	Discussion on Standard Estimation of Arterio-Venous Ratio (AVR)	27
4.4	Performance Analysis	28

	4.5	Future Work	35
CHAPTER 5:		CONCLUSION AND RECOMMENDATION	36
REFERENCES		37
APPENDIX		40

LIST OF FIGURES

Figure 1.3.1: Microvascular sign of retina [5]	3
Figure 2.1.1.1: Fundus Images of Focal Arteriolar Narrowing (right) and Arteriovenous Nicking (left) [8]	4
Figure 3.3.1: Block diagram of the Proposed Method	12
Figure 3.3.1.1: (a) Original Fundus Image, (b) Red Plane of Fundus Image, (c) Green Plane Fundus Image, (d) Blue Plane Fundus Image	13
Figure 3.3.1.2: (a) Complementary Fundus Image, (b) CLAHE Transformation	14
Figure 3.3.1.3: Fundus Background Mask	15
Figure 3.3.1.4: (a) Existence of Noise (white arrow) before Masking, (b) After Masking	15
Figure 3.3.2.1: Bottom-hat Transformation	16
Figure 3.3.2.2: Top-hat Bottom-hat Transform	17
Figure 3.3.2.3: (a) Filtered Image, (b) Background Image, (c) Resulting Image	18
Figure 4.2.1: Artery and Vein Image	23
Figure 4.2.2: Histogram of (a) Red, (b) Green and (c) Blue of Extracted Vessel (image 37)	24
Figure 4.2.3: Classified blood vessel (Artery-red, Vein-blue) for (a) Image 36 and (b) Image 37	27
Figure 4.4.1: Retinal Background Area	32

LIST OF TABLES

Table 2.1.2.1: AVR for different hypertensive retinopathy stages [3]	6
Table 2.1.2.2: Comparison and Analysis of Related Work	7
Table 3.2.1: FYP I Timeline	Error! Bookmark not defined.
Table 3.2.2: FYP II Proposed Timeline	Error! Bookmark not defined.
Table 4.1.1: Corresponding Fundus Images with Enhanced Blood Vessels Images	20
Table 4.1.2: Corresponding Fundus Images with Extracted Blood Vessels Images	21
Table 4.1.3: Corresponding Fundus Images with Extracted Centerline	22
Table 4.2.1: Red, Green and Blue (RGB) Intensities of Artery and Vein	26
Table 4.2.2: Hue, Saturation and Intensity (HSI) value of Artery and Vein	26
Table 4.3.1: Vessel Width Estimation for Image 36 and Image 37 in VICAVR Database [11]	28
Table 4.4.1: Categorization of TP, FP, TN and FN	29
Table 4.4.2: Value of TP, FP, TN and FN	30
Table 4.4.3: Fraction value of TP, FP, TN and FN	31
Table 4.4.4: Results Evaluation with DRIVE Database	33
Table 4.4.5: Performance Calculation Comparisons	34

CHAPTER 1

INTRODUCTION

1.1 Project Background

Nothing strike faster than the sudden attack of stroke and it is undoubtedly the most prevalent cause of emotional complications and adult handicap. The most prevalent cause of severe disability and death is the assault from stroke [5]. If doctors are able to diagnose the probability of stroke affecting the patient, they could make the necessary arrangements to prevent the sudden assault of stroke and this would greatly save the patient life.

Among all the cardiovascular diseases, hypertension is one of the most reliable indications of the occurrence of stroke [5]. Recent technology has enable doctors to study the retina for the severity of hypertension in the patient. Arteriovenous (AV) nicking is an abnormality in the eye when there is compression of the vein due to the crossing of artery and it is usually caused by hypertensive retinopathy [10].

Arteriovenous nicking, narrowing of retinal arteriolar, increment of tortuosity of vascular, thickening of blood vessel, extravascular lesions (microanuerysms, cotton wool spot), shunt vessels and so on are the ocular effect of hypertension and has been disclosed to be related with brain illnesses and therefore fundus imaging is a prospective tool in diagnosis of stroke [2].

Hypertensive retinopathy is an ailment that causes harm to the eye which is clearly related to high blood pressure. Hypertensive retinopathy result in drastic changes to the retina such as blood vessels narrowing, nicking of artery, leakage of fluid from

vessels, optic disc swelling and existence of exudates [3]. Hypertensive retinopathy can be identified through Arterio-Venous Ratio (AVR) estimation.

Hypertensive retinopathy identification in fundus images has huge prospective as the image analysis time is faster with a lesser cost. Besides that, there are various publicly available databases such as DRIVE and VICAVR which encourage researchers to choose fundus image. The narrowing of arteriolar is inversely associated with hypertension and is typically articulated by AVR. For the AVR computation, segmentation, classification and measurement of blood vessels are needed [1].

In this thesis, emphasis is placed on the retinal vessel extraction towards estimation of AVR value which would be useful for the detection and grading of hypertensive retinopathy based on the grading done by Keith and Wegner (1939) [24].

1.2 Problem Statement

Hypertensive retinopathy classification system has been associated with severity level of systemic hypertension and other systemic conditions. By identifying the presence and severity of hypertensive retinopathy, the probability of stroke assault could be foretold and measures could be taken to prevent the condition from deteriorating. Ophthalmologists would determine presence of hypertensive retinopathy by taking the patient's fundus image and analyze the relevant microvascular sign. Many researches have been conducted to learn the occurrence of vital retinal signs due to hypertensive retinopathy through fundus image analysis.

With the advancement in imaging technology, presence of ailments such as hypertensive retinopathy, diabetes retinopathy and so on could be identified from fundus image processing. However, the reliability and accuracy in imaging algorithm to detect the presence of hypertensive retinopathy microvascular sign (AV nicking) are still low i.e. 64.51% [7]. For higher accuracy, an excellent extraction of blood vessel is vital. The extraction of vessel usually is affected by the presence of noise i.e. salt and pepper noise, Gaussian noise, and grain noise in the original fundus image. Filtering must be done to

eliminate the noise for a clear and precise vessel extraction. Besides that, some of the vessels especially tiny vessels in the fundus image are not apparent and thus contrast of the vessels must be enhanced for good detection and extraction of the vessel. The background of the fundus image (area outside of the fundus boundary) is not totally black (pixel value not 0) and would affect the vessel extraction process. A fundus mask (binary image) could be used to make that area totally black (make pixel value to 0). Through the assessment of the hypertensive retinopathy condition, future endeavor on the creation of stroke prediction model could be realized.

1.3 Objective & Scope of Study

This project aims to identify and extract vessels from fundus image with microvascular signs (refer Figure 1.3.1) which could be used for computation of AVR. Value of AVR should be used for the identification and assessment of hypertension which would be useful for future work in the prediction of stroke. This is because research shows that there is an evident relationship between existence of funduscopy abnormalities due to hypertensive retinopathy and stroke. In this project, the research was mainly focused on the field of image processing and analysis.

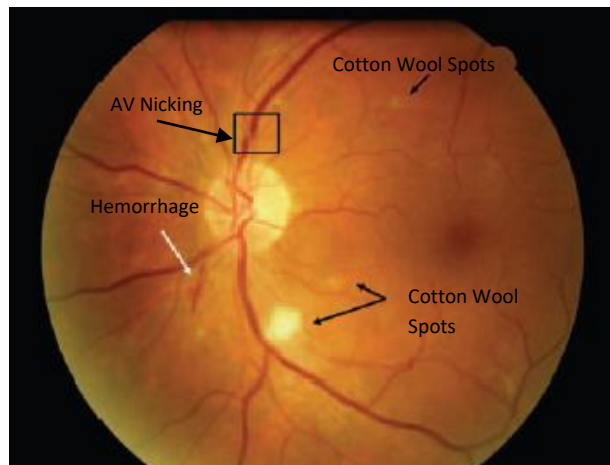


Figure 1.3.1: Microvascular sign of retina [5]

CHAPTER 2

LITERATURE REVIEW

2.1 Related Work

2.1.1 Relationship between Retinal Signs and Stroke

Michelle L. Baker et al. [5] had done a thorough study on the connection between stroke and retinal symptoms. Most retinal symptoms i.e. hypertensive retinopathy, retinal arteriolar emboli and diabetic retinopathy discussed in this paper are related to occurrence of stroke. Retinal signs (i.e. arterio-venous (AV) nicking and narrowing of arteriolar) due to hypertensive retinopathy are mostly related to assault from stroke. Based on Michelle L. Baker [5] hypertensive retinopathy signs are more convincing and consistent precursor of the risk of stroke.

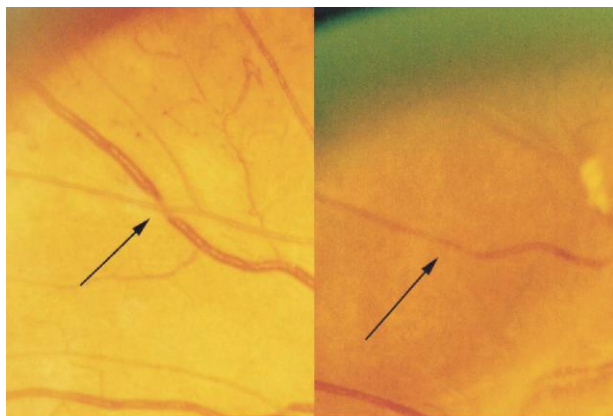


Figure 2.1.1.1: Fundus Images of Focal Arteriolar Narrowing (right) and Arteriovenous Nicking (left) [8]

According to Tien Yin Wong et al. [8], there is an evident relationship between retinal signs (i.e. swelling of optic disc and hemorrhage) and stroke even

when factors affecting risk of stroke and blood pressure were taken into consideration. Based on a study conducted in Gothenburg, Sweden, men with age of 50 with the presence of hypertensive retinopathy signs such as AV nicking and focal arteriolar narrowing (shown in Figure 2.1.1.1) would have an increased in cardiovascular mortality especially stroke [8].

Morillas P, Pallarés V et al. [12] conducted a study which included 887 patients with hypertension (≥ 65 years) to compute the CHADS₂ score to estimate stroke possibility. CHADS₂ score are based on 5 factors (i.e. Congestive heart failure, Hypertension age ≥ 75 , Diabetes mellitus, and prior Stroke attack) which amount to a total of 7 points (2 points for stroke section). It was found that CHADS₂ score is typically used for stroke prediction in patient with hypertension [12].

2.1.2 Hypertensive Retinopathy and Arterio-Venous Ratio (AVR)

According to Uyen T. V. Nguyen et al. [10], studies have shown that AV nicking is greatly related to the presence of hypertension and stroke. They suggested a computer method of identifying the AV nicking severity based on artery-vein crossing in colour retinal images. Multi-scale line detection technique was used to extract the vascular network. The technique proposed is tested on 69 AV crossover points from Singapore Malay Eye Study (SiMES) retinal images. The algorithm used has an accuracy of (96.67%) for the classification of artery and vein. However, an accuracy of 100% is necessary for accurate detection of AV nicking.

K. Narasimhan et al. [3] proposed an approach the identification of blood vessels through top hat transform and median filter on 76 fundus images from VICAV and 25 clinically obtained fundus images. The approach had the advantage of grading the severity of hypertensive retinopathy through the Arterio-Venous Ratio (AVR). Computation of AVR which would be used for defining the severity of hypertensive retinopathy as shown in Table 2.1.2.1 was done through vessel width approximation method. They had utilized Keith and Wegner (1939) [24] grading to

grade the hypertensive retinopathy into four grades i.e. grade 1 (mild hypertensive retinopathy), grade 2 (moderate hypertensive retinopathy), grade 3 (grade 1 and grade 2 combined) and grade 4 (accelerated hypertensive retinopathy) as shown in Table 2.1.2.1. Algorithm used managed to identify 22 out of 25 healthy fundus images and 72 out of 76 fundus images with hypertensive retinopathy.

Table 2.1.2.1: AVR for different hypertensive retinopathy stages [3]

Severity of Hypertensive Retinopathy	AVR	A/V Crossings
Normal	0.667-0.75	None
Grade 1	0.5	Mild compression of venules
Grade 2	0.33	Compression or elevation of venules
Grade 3	0.25	Right angled crossing of vessels, nicking
Grade 4	Fine cords	All above symptoms and distal congestion

Behdad Dashtbozorg et al. [1] presented an automated technique on artery/vein (A/V) for detecting the changes in vasculature as well as computation of distinctive signs related to hypertension using the evaluation of graph obtained from the retinal vessels. Outcome of this approach is compared and tested with manual labeling for the three different databases i.e. VICAVR, INSPIREAVR and DRIVE with an accuracy of 89.8%, 88.3% and 87.4% based on the acquired images from mentioned databases respectively. Mohammed Al-Rawi et al. [4] applied matched filters for the identification of blood vessels. The result of the algorithm was tested using DRIVE database. Roy P. K et al. [7] suggested a method to classify the AV nicking severity automatically based on retinal venular width analysis where the width was computed using both intensity and edge information. The proposed technique was tested on 93 AV crossover points which had been categorized by two distinguished ophthalmologists into 4 classes. This method yielded an accuracy of 64.51% in classifying AV nicking level of severity when compare to the contemporary method [22].

Manikis et al. [5] utilized a hessian based vessel extraction approach as well as thresholding. The result was tested on STARE and DRIVE databases. Unfortunately, technique used for optic disc localization was not discussed in detail. Table 2.1.1 shows the reviewed research papers for the related work in hypertensive retinopathy. It is vital to have a holistic review on all the relevant papers to save times of dealing with the same problems encountered by the previous researchers. The methods used in all those papers are noted to facilitate in the decision making of which methods would be more suitable. The merit and demerit parts of the research papers are vital to provide a clear guidance on how those problems could be tackled.

Table 2.1.2.2: Comparison and Analysis of Related Work

No	Writer	Year	Title	Techniques used	Implementation	Advantages	Disadvantages
1	K.Narasimhan*, V.C.Neha, K.Vijayarekha [3]	2012	Hypertensive Retinopathy Diagnosis from Fundus Images by Estimation of AVR	Vessel width estimation (median filter, top hat transform)	Diagnosis of hypertensive retinopathy stages	Computing A/V ratio and determining the stages of hypertensive retinopathy	No grading even with a large set of data
2	Behdad Dashtbozorg, Ana Maria Mendonça and Aurélio Campilho [1]	2013	An Automatic Graph-Based Approach for Artery/Vein Classification in Retinal Images	Retinal vasculature graph examination	Classification of artery or vein in retinal	Able to classify whole retinal vasculature and not limited to specific region of interest	No substantive assessment of hypertensive retinopathy
3	Michelle L. Baker, Peter J. Hand, Jie Jin Wang, Tien Y. Wong [5]	2008	Retinal Signs and Stroke (Revisiting the Link Between the Eye and Brain)	Analysis of hypertensive retinopathy and diabetic retinopathy signs	Prediction of stroke based on hypertensive retinopathy and diabetic retinopathy	Utilizing retinal signs to anticipate the probability of stroke	Lack of imaging processing methods on the fundus image for determining hypertensive retinopathy
4	Pallab Kanti Roy, Uyen T. V. Nguyen, Alauddin Bhuiyan and Kotagiri Ramamohanarao [7]	2014	An Effective Automated System for Grading Severity of Retinal Arteriovenous Nicking in Colour Retinal Images	Vein width computation based on edge information and intensity of the vein	Analyzing AV nicking level of severity	Improved classification accuracy (64.51%) compared to classification accuracy (49.46%) by recent method [22]	Mediocre classification accuracy
5	Uyen T. V. Nguyen, Alauddin Bhuiyan, Laurence A. F. Park, Ryo Kawasaki, Tien Y. Wong, Jie J. Wang, Paul Mitchell, Kotagiri Ramamohanarao [10]	2013	Automated Quantification of Retinal Arteriovenous Nicking from Colour Fundus Images	Multi-scale detection Artery-vein identification	Devise a computer method for detection of AV nicking automatically	High (96.67%) artery-vein identification and provide link between AV nicking with systemic and eye diseases	Insufficient correlation data on hypertensive retinopathy and stroke
6	Tien Yin Wong, Ronald Klein, Barbara E. K. Klein, James M. Tielsch, Larry Hubbard and F. Javier Nieto [8]	2001	Retinal Microvascular Abnormalities and their Relationship with Hypertension, Cardiovascular Disease, and Mortality	Reviewing methods used in measuring retinal vessel width	Clinical implication of retinal microvascular abnormalities	Provide a detailed relationship between abnormalities of microvascular in retina with stroke and hypertension	Lengthy and no new imaging techniques for fundus image

2.2 Critical Analysis

From all the studies reviewed, AVR is a crucial element in the identification and grading of hypertensive retinopathy. AV nicking (precursor for stroke and hypertensive retinopathy) [7] plays a vital role as well in the identification of hypertensive retinopathy as various retinal microvascular abnormalities such as hemorrhage, swelling of optic disc and exudates are present in other cardiovascular diseases such as diabetic retinopathy. Therefore, existence of hypertensive retinopathy can be confirmed with the existence of AV nicking. Uyen T. V. Nguyen et al [10] method of artery-vein identification (accuracy of 96.67%) would be useful in the estimations of both AV nicking and AVR as both estimations required artery to be distinguished from vein.

Through all the paper reviewed, generally three main steps (vessels extraction, vessels classification and vessels width measurement) were required to detect hypertensive retinopathy. AVR computation would be the key element for the identification of hypertensive retinopathy. Besides that, AVR value also could be used to grade the severity of hypertensive retinopathy. However, Keith and Wegner (1939) [24] grading used were not scientifically proven and certified although the grading was acknowledged by most practitioners. In this research, emphasis would be placed on the extraction of the blood vessel from fundus image.

In the future work of stroke prediction, CHADS₂ score could be used with several modifications where more emphasis should be placed on the hypertension as it is a vital and proven tool for stroke estimation in patients with nonvalvular atrial fibrillation [12]. CHADS₂ score was chosen due to its simplicity as it requires 5 factors (i.e. heart failure, high blood pressure, lifespan, diabetes and stroke) only to predict stroke probability. Nevertheless, modification should be done in the future to simplify this score where only hypertension should be required for predicting stroke.

CHAPTER 3

METHODOLOGY

3.1 Process Methodology

Problems identification was done on the research project based on the objectives. To further deepen the understanding of the research topic, literature review was done where numerous credible research papers on the topic of retinal vasculature were studied and reviewed. This is a vital step to provide an exposure on the research focus and ease future endeavor on completing the research.

Once multiple research papers were reviewed, critical analysis was done to grasp the core of the problems and ideas on tackling the problems. This step also provides the strong and weak point of the previous researches done which facilitates in the modification and enhancement stage. The next step would be creating the project milestone and Gantt chart to ease the flow of the project. This step would help in time management and reduce unexpected roadblocks during the project completion.

Relevant data was of utmost importance in a research so that the researchers could test their hypothesis and theory. Therefore, the subsequent step would be finding the important data and fundus images. Fundus images are divided into two sections where the first section would be normal fundus images while the other would be fundus images of people with hypertensive retinopathy. Imaging techniques learnt would be implemented on the fundus images to extract out important region from the fundus. Algorithm would be used to ensure successful fundus images analysis.

3.2 Gantt Chart & Key Milestones

Table 3.2.1 and 3.2.2 are the timeline (Gantt chart) with the important milestones for both FYP I and FYP II respectively.

Table 3.2.1: FYPI Timeline

No	Tasks	FYP 1 (Week)													
		1	2	3	4	5	6	7	8	9	10	11	12	13	14
1	Literature Review	■	■	■	■	■	■	■	■	■	■	■	■	■	■
2	Methods Identification					■	■	■	■	■	■	■	■	■	■
3	Gathering of fundus image databases (VICAVR, DRIVE, HRF)						■	■						■	■
4	Digital image processing learning								■	■	■	■	■	■	■
5	Testing of different proposed methods									■	■	■	■	■	■
6	Finalize on the method to be used for the research											■			
7	Color extraction and morphological operation of fundus image											■			
8	Fundus image enhancement												■		
9	Creation of mask for fundus image													■	
10	Basic image preprocessing model (Matlab)													■	■
11	Documentation														
	Extended proposal							●							
	Proposal Defense & Progress Evaluation										●				
	Interim & Final Report													●	●

● Key milestone

■ Process

Table 3.2.2: FYP II Proposed Timeline

No.	Tasks	FYP II (Week)														
		1	2	3	4	5	6	7	8	9	10	11	12	13	14	15
1	Vessel enhancement algorithm	■														
2	Feature extraction algorithm for vessel identification		■													
3	Identification of artery and vein			■	■	■	■	■	■	■	■	■	■	■		
4	Estimation of vessel width and AVR ratio						■	■	■	■	■	■	■	■		
5	Hypertensive retinopathy identification model											■	■	■		
6	Implementation of the model								■	■	■	■	■	■	■	
7	Testing the algorithm											■	■	■	■	
8	Poster Presentation										●					
9	Project Viva															●
10	Documentation															
	Progress Report									●						
	Draft Final Report													●		
	Dissertation (soft copy)														●	
	Technical Paper														●	
	Viva															●
	Dissertation (hard copy)															●

● Key milestone
 ■ Process

3.3 Approach Overview

The color fundus images were obtained from online DRIVE [6] and VICAVR [11] databases. Photographs from DRIVE have been obtained through a Cannon CR5 non-mydratiac 3CCD camera with a resolution of 768x584. Images from VICAVR were obtained via a non-mydratiac camera (TopCon NW-100) at 768 by 584 pixels [11]. All the images from VICAVR were labelled by three experts in terms of vessels caliber and type (artery/vein).

The labelling done by the experts were vital to compare and calculate the accuracy of this approach. In this research, an approach was proposed to extract vessel from fundus image which could be used to compute the Arterio-Venous Ratio (AVR) value to assess the presence and severity of hypertensive retinopathy. Four major stages were required for the implementation of this approach i.e. preprocessing, vessels extraction, vessels classification and vessels caliber measurement. Figure 3.3.1 illustrates the block diagram of the overall structures of the proposed approach. However, the algorithm for the last two stages for the proposed approach i.e. artery/vein classification and AVR estimation were not completed successfully in this research.

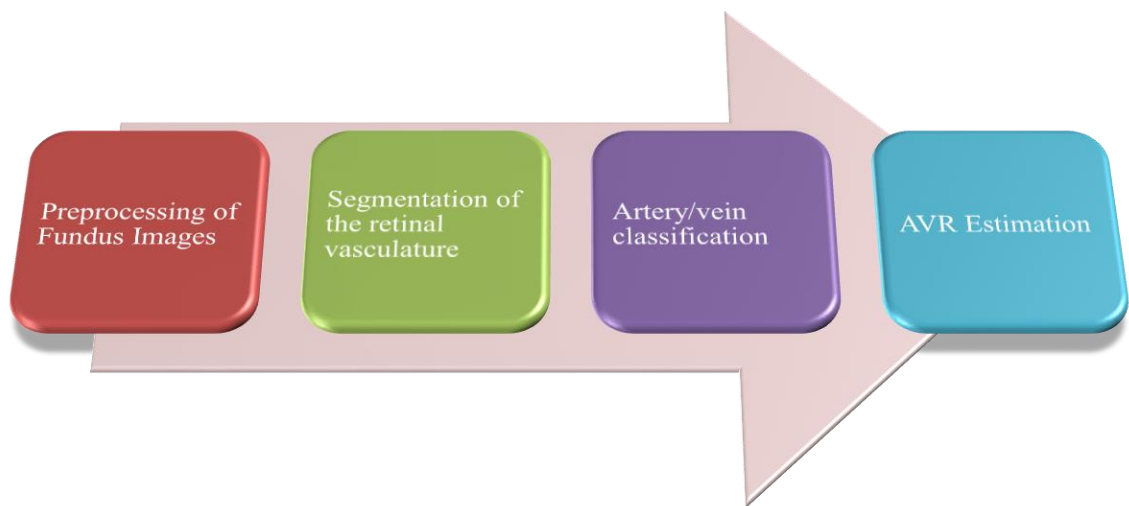


Figure 3.3.1: Block diagram of the Proposed Method

3.3.1 Preprocessing of Fundus Image

Preprocessing of fundus images are implemented beforehand to ensure all the fundus images are uniform which would ease further processing and improve accuracy. In addition, preprocessing of fundus image will eliminate the background noise and enhance the image i.e. contrast for easier and better processing in the subsequent stage. In the preprocessing stage, the green intensity from the fundus image is separated to acquire a monochrome image.

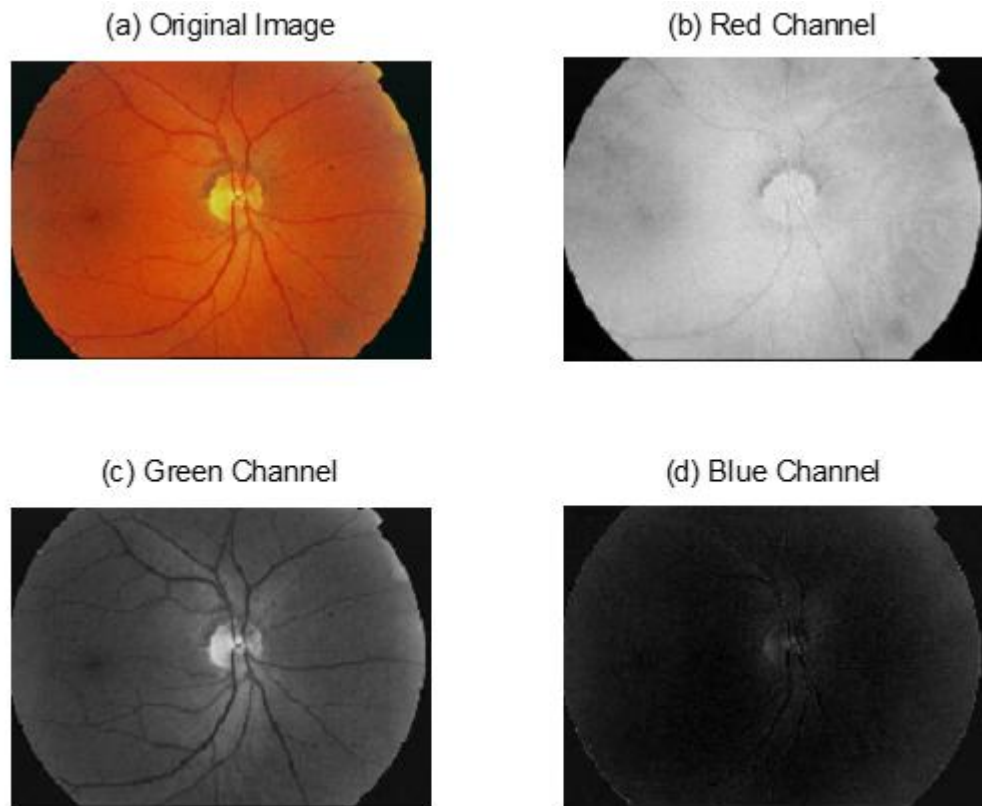


Figure 3.3.1.1: (a) Original Fundus Image, (b) Red Plane of Fundus Image, (c) Green Plane Fundus Image, (d) Blue Plane Fundus Image

Figure 3.3.1.1 shows how the red, green and blue planes are acquired from the input fundus image. Green channel is chosen because green channel produces the best contrast (high intensity) for vessel compared to red which would make the vessel more prominent, while blue has a short dynamic range which would make the whole image darker and difficult to locate blood vessel. Besides, by extracting green channel most features are visible while in red channel only boundary is visible and

high presence of noise in the blue channel [17]. As we can see from Figure 3.3.1, separating green channel from the fundus image will make the blood vessel darker than the background and easier to identify. Formula for green channel extraction is

$$G_c = \frac{G_i}{R_i + G_i + B_i} \quad (1)$$

Where G_c is green channel R_i , G_i and B_i are red, green and blue intensity respectively [20].

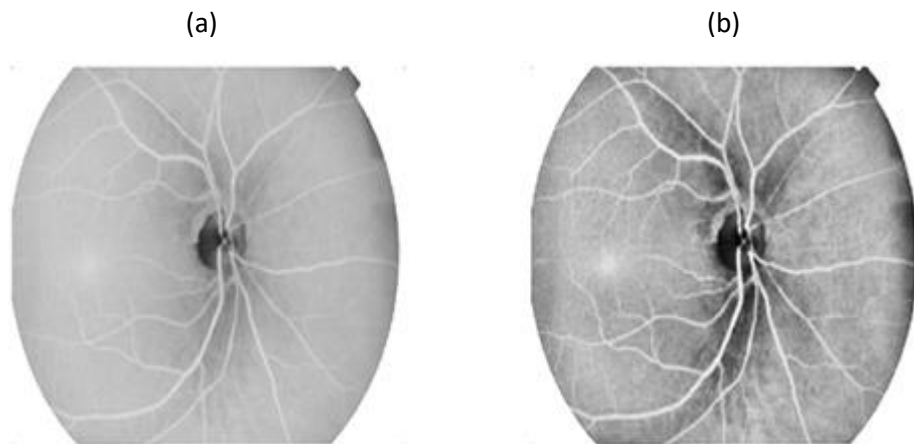


Figure 3.3.1.2: (a) Complementary Fundus Image, (b) CLAHE Transformation

After extracting the green channel, complement function was used to enhance the retinal blood vessels as blood vessels are lighter than background. Median filtering with a 3x3 pixel neighborhood mask size was done to smoothen the fundus image prior to further processing. Histogram equalization function was utilized for improving the contrast of the complementary image. Figure 3.3.1.2 shows the fundus image that undergoes complement CLAHE functions where the image contrast was drastically improved making the edges i.e. blood vessels more evident which would greatly ease the detection of edges.

Contrast-Limited Adaptive Histogram Equalization (CLAHE) technique was performed with the aim to enhance the image contrast where transformation was made to the image pixels in such a way that output histogram similar to the defined histogram. CLAHE would make the image details to be more prominent as it improves the global contrast and avoid over amplification of noise which would be useful for edges improvement [14].

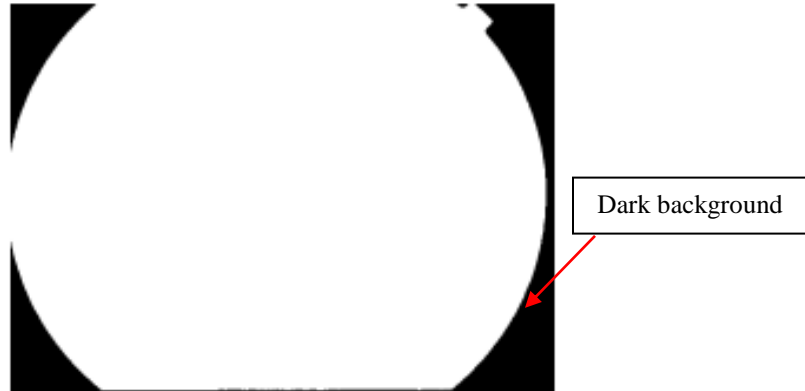


Figure 3.3.1.3: Fundus Background Mask

Creation of fundus mask is vital so that the boundaries structure of the image could be displayed [17]. A fundus background mask was created by extracting the red channel and thresholding was applied before converting it to binary image as shown in Figure 3.3.1.3 which would be used to eliminate the dark background noise from the green channel. Masking was also necessary for the subsequent transformation as the existence of noise in the dark background would be eliminated by the fundus mask when morphology operation i.e. top-hat transform was utilized as shown in Figure 3.3.1.4. This is necessary as the noise would be present in the vessel extraction stage if not removed. Figure 3.3.1.4(b) shows the result after the dark background noise (white arrow) is eliminated through masking.

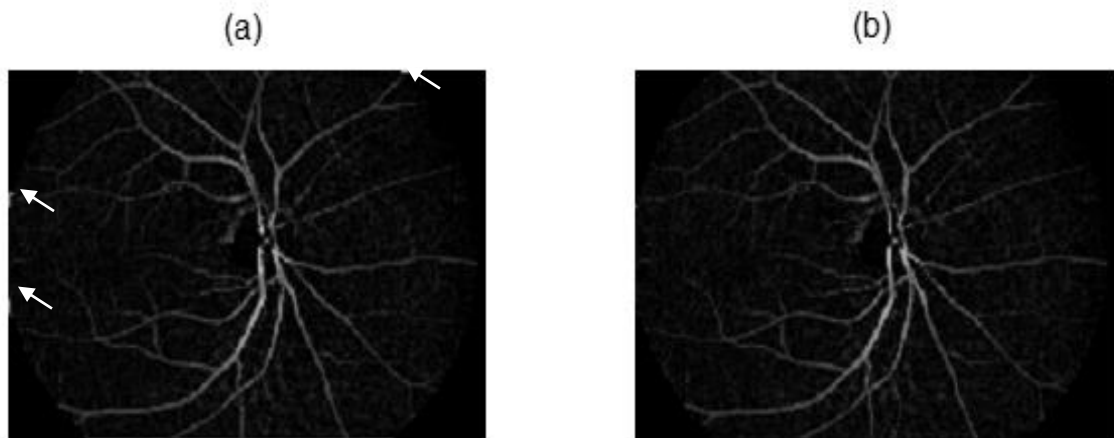


Figure 3.3.1.4: (a) Existence of Noise (white arrow) before Masking, (b) After Masking

3.3.2 Extraction of Blood Vessels

After performing CLAHE transformation, the resulting image was morphologically transformed using top-hat approach with a disk-shaped (radius = 8 pixels) structuring element. Top hat transform was performed to acquire tiny, bright details i.e. vessel by enhancing bright components and remove other components that are bigger than the structuring element from the fundus image and at the same time correct uneven illumination. Figure 3.3.1.4(b) shows the result after performing top-hat filtering and it could be seen that only vessel was extracted while the other regions in the image was concealed.

Besides that, bottom-hat transformation with a disk-shaped (radius = 8 pixels) structuring element was also implemented to the fundus image (after CLAHE transform). Bottom-hat operation has the opposite effect of top-hat operation as it enhances dark components in a bright background. Figure 3.3.1.5 shows the resulting image due to bottom hat filtering. In general, both top-hat and bottom-hat transforms were used to remove components that are larger than the structuring element. Result of bottom-hat transformation (Figure 3.3.1.5) would be deducted from the previously acquired top-hat transformed image (Figure 3.3.1.4(b)) and are shown in Figure 3.3.1.6. This subtraction was done to remove other details i.e. not vessel from the image.

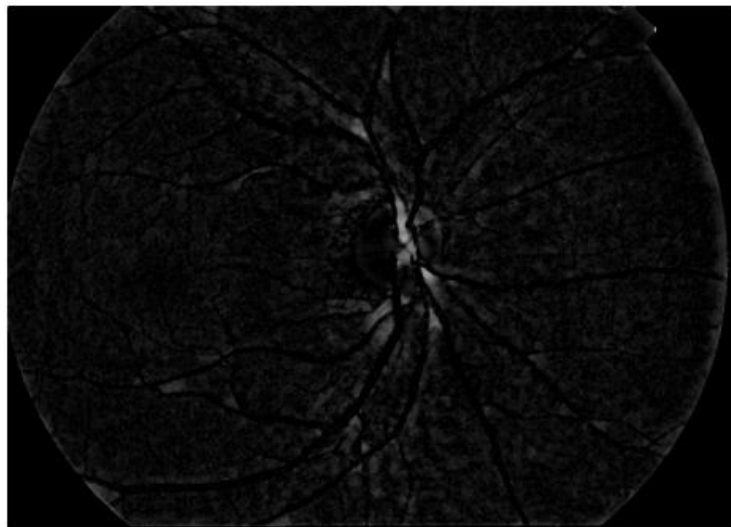


Figure 3.3.2.1: Bottom-hat Transformation

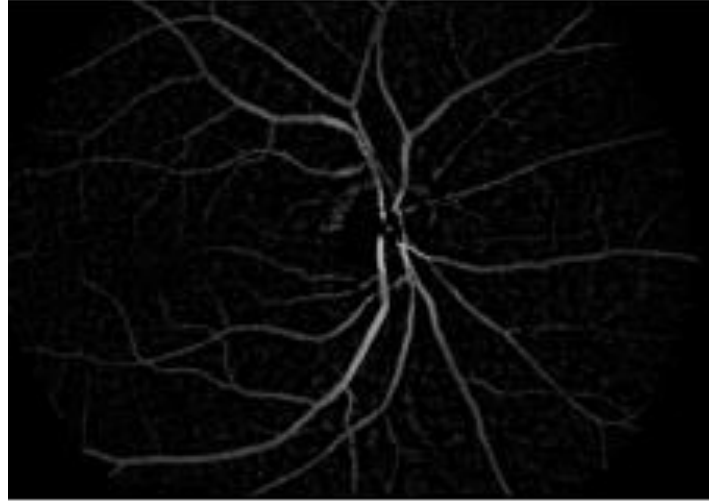


Figure 3.3.2.2: Top-hat Bottom-hat Transform

After performing top-hat bottom-hat transform and acquired resulting image (Figure 3.3.2.2), morphological open function with a structuring element of disk of 15 pixels radius was applied to the filtered image for background removal. By performing morphological opening, tiny elements from the foreground was eliminated and placed in the background. Any component that is larger than the structuring element was removed resulting in Figure 3.3.2.3(b). Figure 3.3.2.3(a) shows the image after top-hat and bottom-hat transforms while Figure 3.3.2.3(b) shows the image after morphology opening where subtraction would be performed to both image for background removal.

Figure 3.3.2.3(c) shows the resulting image (with adjustment done to the vessel intensity) due to the subtraction of both images in Figure 3.3.2.3(a) and (b). For Figure 3.3.2.3(c), the intensity was adjusted in such a way that there is a 1% saturation of data at small and large intensity value of the selected image. Therefore, the intensity of the vessel was increased albeit with some noise to make the vessel more apparent. This adjustment to the intensity would enable easier and better extraction of the vessels as it made the vasculature more prominent and apparent for thresholding. The next step for the vessel extraction would be the computation of the threshold value of the gray level.

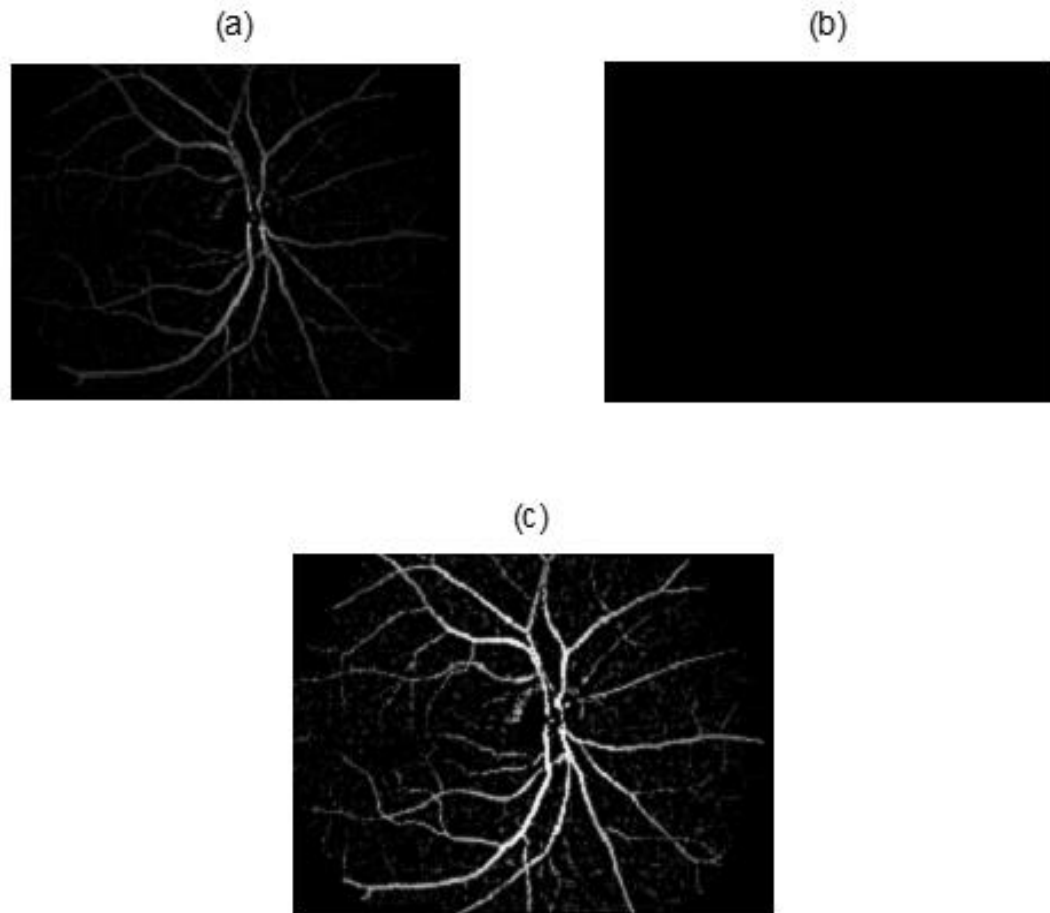


Figure 3.3.2.3: (a) Filtered Image, (b) Background Image, (c) Resulting Image

Thresholding is a method typically used to convert grayscale image into a binary image where a black pixel replacement will be done to the image if the intensity is lower than certain value or threshold and if exceed the threshold or value, a white pixel will be used for replacement i.e. binary 1(white) and binary 0 (black). For the threshold computation, Otsu's method was implemented as the function for performing Otsu's method of thresholding is available in Matlab. Otsu's method would execute thresholding based on clustering methods i.e. gray intensities sections are grouped into 2 components (foreground and background). Once the threshold value of image from Figure 3.3.2.3(c) was calculated, binarization process would be done followed by removal of small components from the resulting binary image. Any components fewer than 30 pixels were removed from the image during the binarization process.

CHAPTER 4

RESULT AND DISCUSSION

4.1 Extracted Vessel

The approach implemented was compared and tested on both VICAVR and DRIVE databases. Four images were arbitrarily selected to demonstrate the results of the approach. Table 4.1.1 shows the result of the fundus images after the blood vessels were enhanced. The intensities of the vessels were adjusted through pixel scaling to improve the vessels. However, this result in some background noise as the noise was also amplified at the same time.

The presence of noise in the enhanced images would not greatly affect the result of vessel extraction as thresholding would be done to eliminate the noise and convert the image into binary form. Improvement can still be done to the proposed approach so that the noise generated during pixel scaling could be greatly diminished creating a more ideal enhanced blood vessel image.

Table 4.1.2 shows the fundus images of the extracted blood vessels. The limitation of this approach is the inability to extract tiny vessels completely which result in some discontinuity of the vasculature. Nonetheless, this would not have an adverse effect on the overall performance of the algorithm. For better extraction, modification could be done to the thresholding so that all the vessels (including tiny vessels) could be extracted during the binarization process. Table 4.1.3 shows the extracted centerline of the fundus image. Improvement could be done to the skeletonization process to improve the extracted centerline. Besides that, the result of the extracted centerline is related to the result of the extracted vessels.

Table 4.1.1: Corresponding Fundus Images with Enhanced Blood Vessels Images


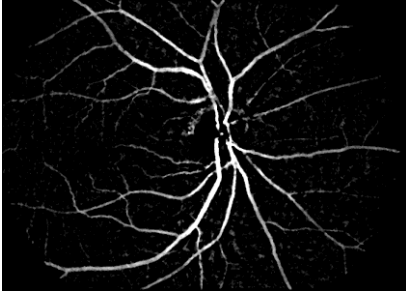
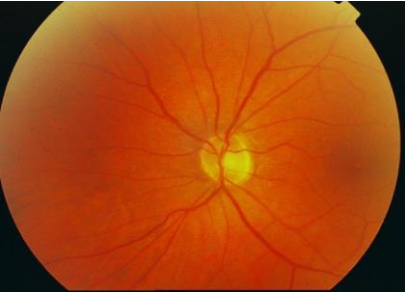
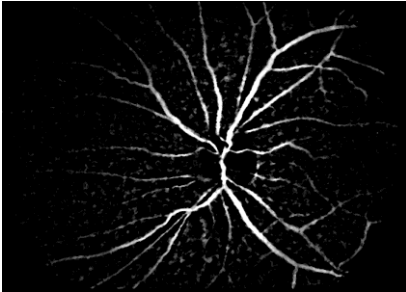
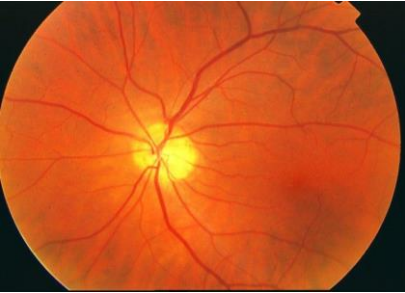
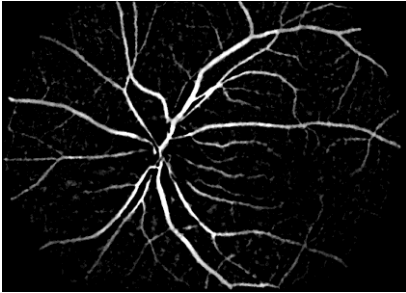

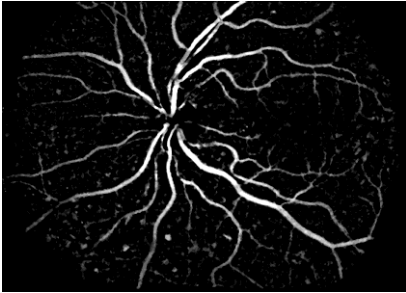
NO	FUNDUS IMAGES	ENHANCED BLOOD VESSELS IMAGES
1	 A fundus photograph showing the optic disc and a network of retinal blood vessels. The vessels are thin and somewhat faint against the orange-red background of the retina.	 The corresponding enhanced fundus image where the blood vessels are highlighted in white against a black background, making them much more prominent and easier to trace.
2	 A fundus photograph showing the optic disc and a network of retinal blood vessels. The vessels are thin and somewhat faint against the orange-red background of the retina.	 The corresponding enhanced fundus image where the blood vessels are highlighted in white against a black background, making them much more prominent and easier to trace.
3	 A fundus photograph showing the optic disc and a network of retinal blood vessels. The vessels are thin and somewhat faint against the orange-red background of the retina.	 The corresponding enhanced fundus image where the blood vessels are highlighted in white against a black background, making them much more prominent and easier to trace.
4	 A fundus photograph showing the optic disc and a network of retinal blood vessels. The vessels are thin and somewhat faint against the orange-red background of the retina.	 The corresponding enhanced fundus image where the blood vessels are highlighted in white against a black background, making them much more prominent and easier to trace.

Table 4.1.2: Corresponding Fundus Images with Extracted Blood Vessels Images



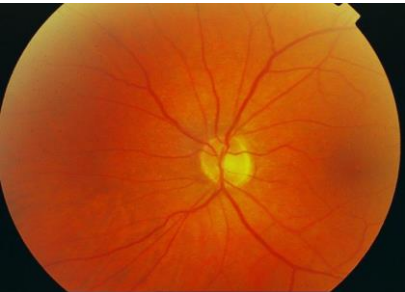
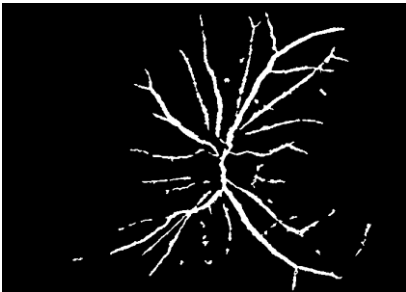

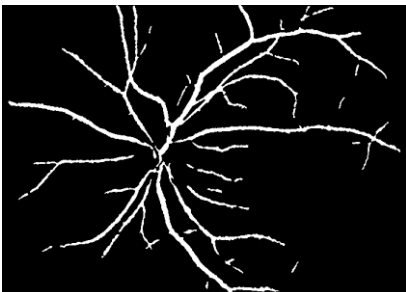

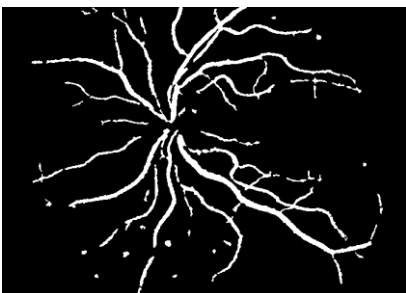
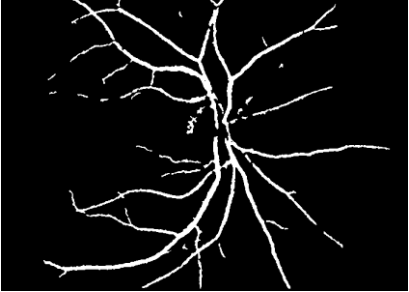
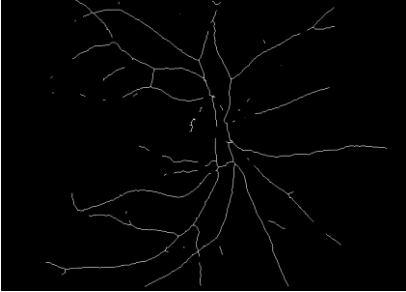
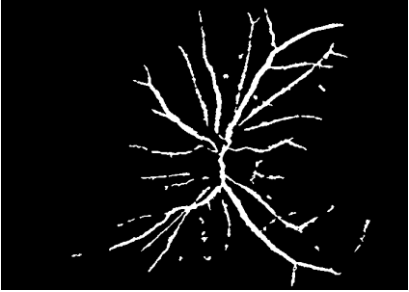
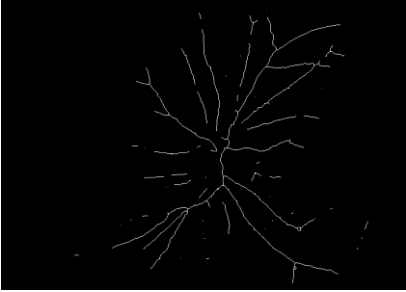
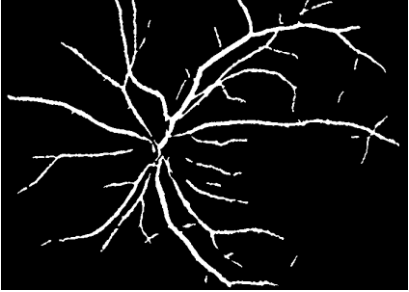
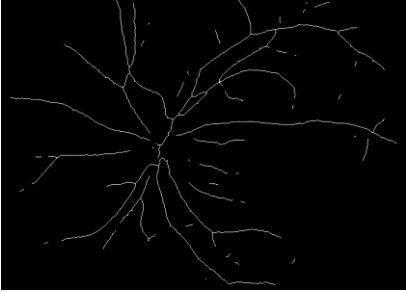

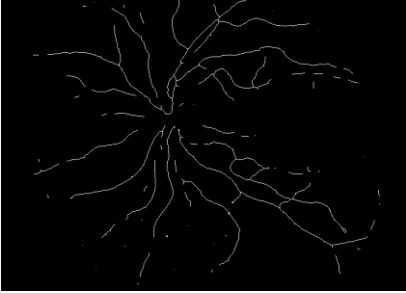
NO	FUNDUS IMAGES	EXTRACTED BLOOD VESSELS IMAGES
1	 A fundus image showing the retina with a central optic disc and a network of blood vessels.	 A binary image showing the extracted blood vessels from the fundus image, appearing as white lines on a black background.
2	 A fundus image showing the retina with a central optic disc and a network of blood vessels.	 A binary image showing the extracted blood vessels from the fundus image, appearing as white lines on a black background.
3	 A fundus image showing the retina with a central optic disc and a network of blood vessels.	 A binary image showing the extracted blood vessels from the fundus image, appearing as white lines on a black background.
4	 A fundus image showing the retina with a central optic disc and a network of blood vessels.	 A binary image showing the extracted blood vessels from the fundus image, appearing as white lines on a black background.

Table 4.1.3: Corresponding Fundus Images with Extracted Centerline

NO	EXTRACTED BLOOD VESSELS IMAGES	EXTRACTED CENTERLINE
1	 A binary image showing a dense network of white blood vessels on a black background. The vessels are thick and form a complex, branching structure.	 A binary image showing the centerlines of the blood vessels from the first image. The vessels are represented as thin, single-pixel-wide white lines on a black background.
2	 A binary image showing a network of white blood vessels on a black background. The vessels are thick and form a complex, branching structure.	 A binary image showing the centerlines of the blood vessels from the second image. The vessels are represented as thin, single-pixel-wide white lines on a black background.
3	 A binary image showing a network of white blood vessels on a black background. The vessels are thick and form a complex, branching structure.	 A binary image showing the centerlines of the blood vessels from the third image. The vessels are represented as thin, single-pixel-wide white lines on a black background.
4	 A binary image showing a network of white blood vessels on a black background. The vessels are thick and form a complex, branching structure.	 A binary image showing the centerlines of the blood vessels from the fourth image. The vessels are represented as thin, single-pixel-wide white lines on a black background.

4.2 Discussion on Standard Artery and Vein Classification

Typically, artery is thinner and brighter than vein and this is because artery has higher central reflex and this is especially true in fundus image with hypertensive retinopathy. Figure 4.2.1 shows the image of both vein and artery where vein appear darker than artery. Besides, vein is also thicker than artery. This is an important feature for the blood vessels classification. The mean and standard deviation of vessel pixels were important features for the classification.

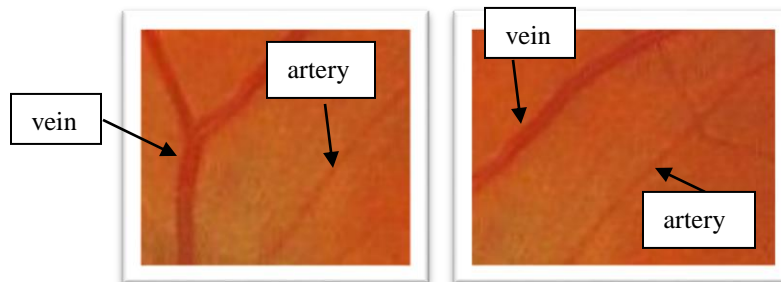
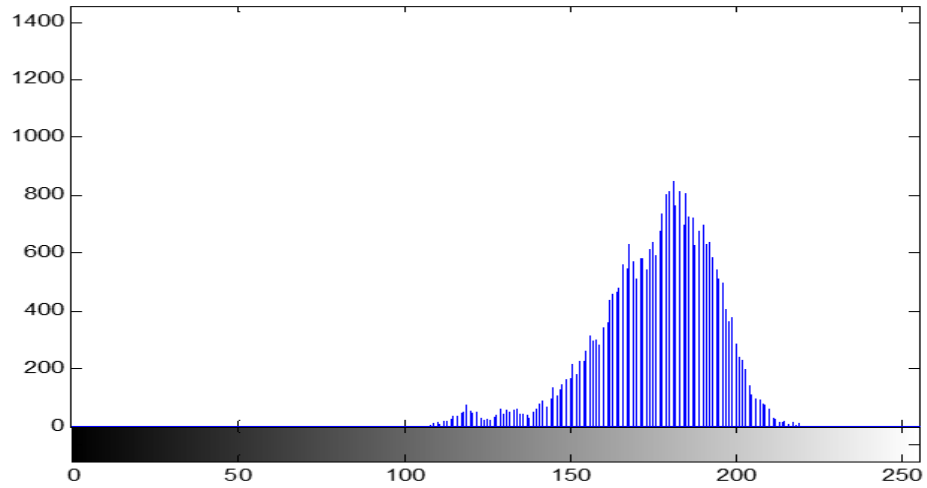


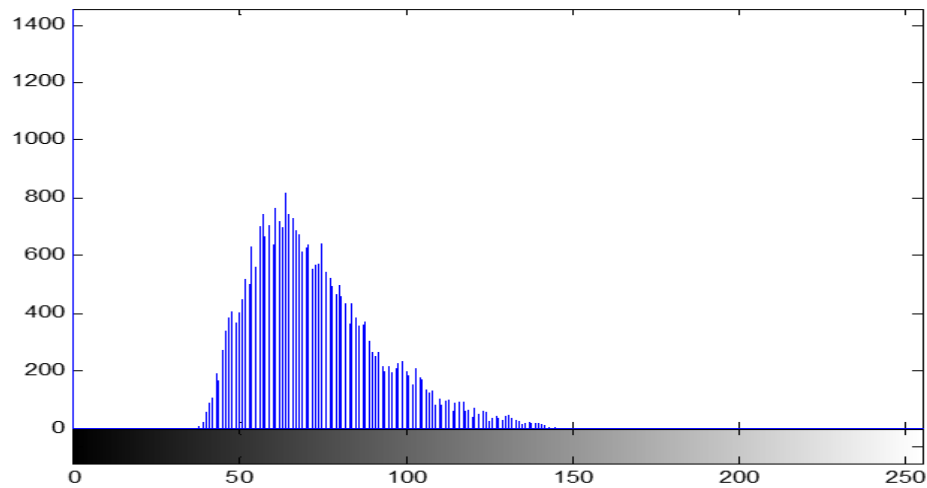
Figure 4.2.1: Artery and Vein Image

The blood vessels segmented should classified into arteries and veins and thus an accurate blood vessels classification was crucial as the effects of hypertensive retinopathy to arteries and veins vary. The point of entry of main blood vessels are located at the optic disc region. Due to timing constraint, automated classification was not created and only 2 fundus images from VICAVR (image 36 and image 37) were selected for the classification as the features are more apparent and vessel type was labelled by first expert from medical institution [11]. To classify blood vessel into artery or vein, the features extracted were based on features used by Dashtbozorg [1].

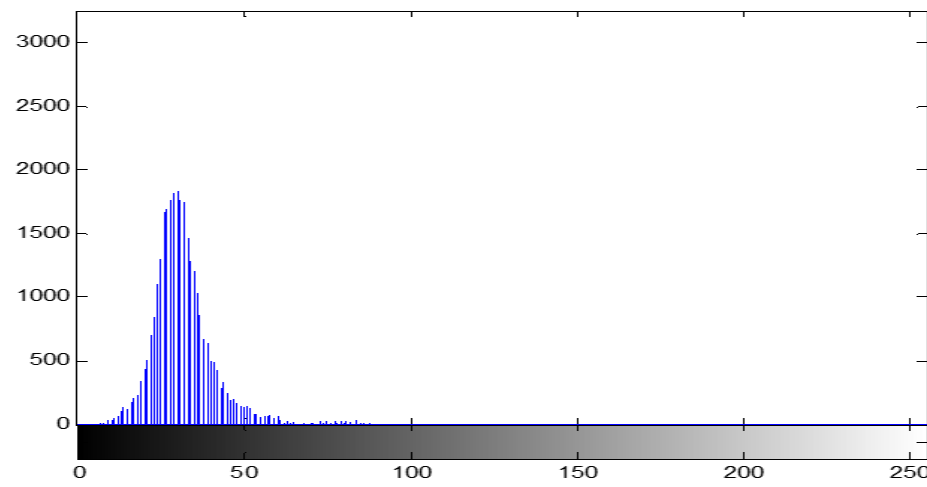
- Red, Green and Blue intensities of extracted vessel
- Saturation, Hue and Intensity of extracted vessel
- Vessel mean intensities of Red, Green and Blue
- Vessel mean intensities of Hue, Saturation and Intensity
- Vessel standard deviation of Red, Green and Blue intensities
- Vessel standard deviation of Hue, Saturation and Intensity
- Vessel maximum and minimum intensities of Green and Red channels



(a)



(b)



(c)

Figure 4.2.2: Histogram of (a) Red, (b) Green and (c) Blue of Extracted Vessel (image 37)

Figure 4.2.2 shows the histogram of Red, Green and Blue of extracted vessel from VICAVR (image 37). The maximum red intensities for the extracted vessels are 207 (image 36) and 226 (image 37) while the minimum red intensities are 90 (image 36) and 108 (image 37). Maximum green intensities are 147 (image 36) and 149 (image 37) while minimum green intensities are 24 (image 36) and 37 (image 37). Based on the observation made, it was found that most arteries occupied the top 20% of the maximum red intensity while most veins are located below the top 20% of the maximum red intensity. From Figure 4.2.2, the pixels that occupied the top 20% of the maximum red intensity were lesser because veins are thicker and occupied more pixels than arteries. Besides that, arteries color channels i.e. red, green and blue intensities usually are larger than veins because arteries are brighter while veins are darker.

The mean of red, green and blue intensities for the extracted vessels are 149.7554, 51.9931 and 25.6558 (image 36) as well as 175.9211, 72.9174 and 31.9743 (image 37) respectively. The mean of hue, saturation and intensity for extracted vessels are 0.0353, 0.8235 and 0.5852 (image 36) as well as 0.047, 0.6883 and 0.3654 (image 37) respectively. The vessel standard deviation for red, green and blue channels were 0.0588, 0.0853 and 0.0505 (image 36) as well as 0.0763, 0.0706 and 0.0394 (image 37) respectively. The vessel standard deviation for hue, saturation and intensity were 0.0505, 0.0198 and 0.0478 (image 36) as well as 0.022, 0.0669 and 0.0506 (image 37) respectively.

It was observed that most arteries had value larger than the mean of green and blue intensities as well as mean of hue and intensity while most veins had value lower than the mean of hue, intensity, green and blue values. The observations made should be used to classify blood vessel into artery or vein. Table 4.2.1 summarized the extracted intensities of red, green and blue in specific coordinates of different vessel types in two fundus images (image 36 and image 37). Table 4.2.2 summarized the extracted values of hue, saturation and intensity in specific coordinates of different vessel types in two fundus images (image 36 and image 37). The first expert in VICAVR database had labelled several coordinates with the vessel types and three coordinates were selected on each different artery and vein.

Table 4.2.1: Red, Green and Blue (RGB) Intensities of Artery and Vein

Image	X, Y Coordinates (vessel no)		Red		Green		Blue	
	Artery	Vein	Artery	Vein	Artery	Vein	Artery	Vein
36	424, 255 (26)	330, 209 (35)	164	156	65	46	26	18
	314, 229 (32)	395, 210 (36)	167	161	60	42	18	21
	334, 432 (41)	468, 281 (37)	179	156	55	31	34	11
37	381, 214 (46)	397, 410 (0)	191	168	109	54	36	29
	455, 321 (11)	485, 288 (39)	189	178	106	56	38	16
	361, 408 (7)	357, 217 (49)	179	185	88	68	31	35

Table 4.2.2: Hue, Saturation and Intensity (HSI) value of Artery and Vein

Image	X, Y Coordinates (vessel no)		Hue		Saturation		Intensity	
	Artery	Vein	Artery	Vein	Artery	Vein	Artery	Vein
36	424, 255 (26)	330, 209 (35)	0.0423	0.0328	0.8625	0.8782	0.3124	0.2889
	314, 229 (32)	395, 210 (36)	0.0442	0.0226	0.8448	0.8284	0.3490	0.3216
	334, 432 (41)	468, 281 (37)	0.0264	0.023	0.8011	0.9177	0.3608	0.2667
37	381, 214 (46)	397, 410 (0)	0.0785	0.0257	0.8115	0.8047	0.439	0.3346
	455, 321 (11)	485, 288 (39)	0.0772	0.0360	0.8011	0.9257	0.4301	0.3085
	361, 408 (7)	357, 217 (49)	0.0608	0.0336	0.8132	0.8098	0.3974	0.3712

From Table 4.2.1 and Table 4.2.2, artery values for green intensity, blue intensity hue and intensity were above the mean for all these values. Therefore, by specifying the top 20% of maximum red intensity as well as mean values for green, blue, hue and intensity, artery could be classified. Based on the observations made, the features extracted could be fed to classifiers such as (k-NN, LDA, SVM and neural network) to distinguished between vein and artery from the fundus image. In this research, automated approach for this stage was not created due to timing constraint. This stage is

a prerequisite for the final stage i.e. AVR computation. Figure 4.2.3 shows a simple classification done using mean of green intensity to classify blood vessel into artery (red line) or vein (blue line) for image 36 and image 37 in VICAVR database. Overlaying of classified vessel to the labelled images (36 and 37) by first expert were attached in the Appendix. Nonetheless, for better classification previous mentioned observations could be implemented into the classifier such as SVM, LDA and k-NN.

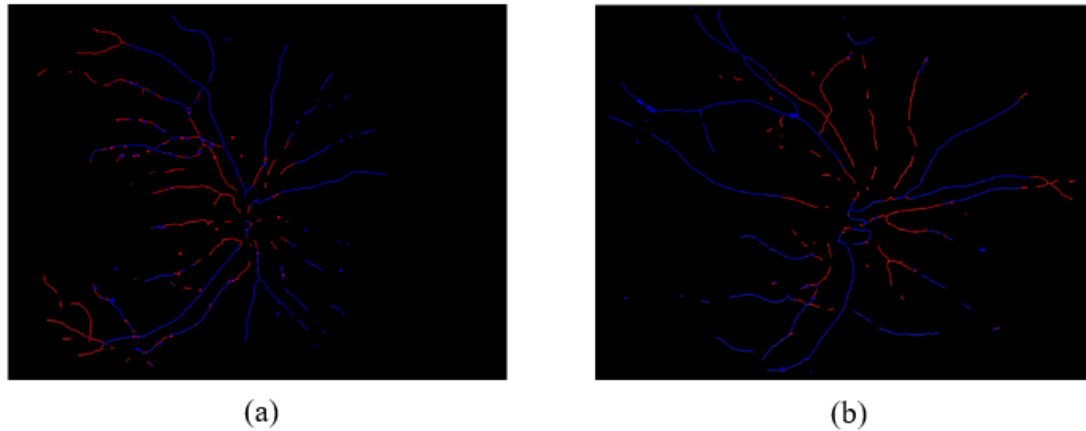


Figure 4.2.3: Classified blood vessel (Artery-red, Vein-blue) for (a) Image 36 and (b) Image 37

4.3 Discussion on Standard Estimation of Arterio-Venous Ratio (AVR)

Alteration in venular caliber is an indication of diseases such as hypertensive retinopathy [3]. The grading used for assessing hypertensive retinopathy should be in accordance with the grading used by K. Narasimhan et al. [3] shown in Table 2.1.2.1. The acquired AVR should be computed based on the mean width of both arteries and veins where any image with AVR less than 0.667 should be classified as hypertensive retinopathy. The diameter of vein and artery should be estimated and AVR could be computed from the estimated values. Euclidean distance transform was implemented to the extracted centerline pixel to approximate the radius of the vessel width [3].

Table 4.3.1 shows the vessel caliber [11] labelled by first expert and approximated vessel width using Euclidean distance transform for image 36 and image 37 in VICAVR database. There is still plenty room for improvement that should be made to vessel width estimation such as better extraction of vessel so that centerline

pixels are more accurate as the result estimated vessel widths were not ideal. In this research, fully automated approach for the classification of artery and vein stage and the computation of AVR value stage was not completed.

Table 4.3.1: Vessel Width Estimation for Image 36 and Image 37 in VICAVR Database [11]

Image	X, Y Coordinates (vessel no)		Labelled vessel width by first expert		Estimated vessel width	
	Artery	Vein	Artery	Vein	Artery	Vein
36	424, 255 (26)	330, 209 (35)	4.845528	6.044902	2	6.3246
	314, 229 (32)	395, 210 (36)	4.021918	6.333801	4	7.2112
	334, 432 (41)	468, 281 (37)	5.264017	4.229671	2	6.3246
37	381, 214 (46)	397, 410 (0)	4.677884	10.952332	4.4722	8.2462
	455, 321 (11)	485, 288 (39)	5.521891	5.287802	4	5.6568
	361, 408 (7)	357, 217 (49)	6.344262	9.084712	6	10

4.4 Performance Analysis

The results of the extracted vessel from the 20 images in DRIVE using proposed algorithm were attached in the Appendix section. Performance of the proposed vessel extraction results were compared with manually extracted vessel results (gold standard) from DRIVE database [6]. For performance analysis, 4 main parameters must be specified i.e. True Positive (TP), False Positive (FP), True Negative (TN) and False Negative (FN). True positive (TP) refers to the correctly identified blood vessels, false positive (FP) refers to the incorrectly identified blood vessels, and true negative (TN) and false negative (FN) refer to the correctly and incorrectly identified non-blood vessel pixels [28].

This means that TP is the amount of correctly matched vessel (i.e. pixel = 1) in both proposed algorithm and gold standard. FP is the amount of incorrectly matched blood vessel i.e. blood vessel is detected (pixel = 1) using the proposed algorithm but in

the gold standard it is non-blood vessel (pixel = 0). TN is the amount of correctly matched non-blood vessel (pixel = 0) in both proposed algorithm and gold standard. FN is the amount of incorrectly matched non-blood vessel i.e. non-blood vessel is detected (pixel = 0) using the proposed algorithm but in the gold standard it is blood vessel (pixel = 1). Table 4.4.1 shows how TP, FP, TN and FN are categorized for performance analysis.

		GOLD STANDARD	
		Blood Vessel (Positive)	Nonblood Vessel (Negative)
EXTRACTED VESSEL	Blood Vessel (Positive)	True Positive (TP)	False Positive (FP)
	Nonblood Vessel (Negative)	False Negative (FN)	True Negative (TN)

Table 4.4.1: Categorization of TP, FP, TN and FN

Table 4.4.2 summarizes the value of TP, FP, TN and FN for the 20 fundus images from DRIVE. Table 4.4.3 shows the fraction value between TP, FP, TN and FN with gold standard from DRIVE. The fraction value for TP was computed by dividing TP value with all pixels with value 1 from extracted vessel. For fraction value for FP, the value obtained was divided with all pixels with value 1 from extracted vessel. The fraction value for TN was computed by dividing TN value with all pixels with value 0 from extracted vessel. For fraction value for FN, the value obtained was divided with all pixels with value 0 from extracted vessel. Formulas for TP, FP, TN and FN as well as the fraction value for TP, FP, TN and FN [27] are

$$TP = \sum(\text{Extracted Vessel (pixel)} \times \text{Gold Standard (pixel)} == 1)$$

$$FP = \sum(\text{Extracted Vessel (pixel)} - \text{Gold Standard (pixel)} == 1)$$

$$TN = \sum(\text{Extracted Vessel (pixel)} + \text{Gold Standard (pixel)} == 0)$$

$$FN = \sum(\text{Extracted Vessel (pixel)} - \text{Gold Standard (pixel)} == -1)$$

$$\text{Fraction of TP} = \frac{TP}{\sum(\text{Extracted Vessel (pixel)} == 1)} \quad (2)$$

$$\text{Fraction of FP} = \frac{FP}{\sum(\text{Extracted Vessel (pixel)} == 1)}$$

$$\text{Fraction of TN} = \frac{TN}{\sum(\text{Extracted Vessel (pixel)} == 0)}$$

$$\text{Fraction of FN} = \frac{FN}{\sum(\text{Extracted Vessel (pixel)} == 0)}$$

Table 4.4.2: Value of TP, FP, TN and FN

Image sequence	True Positive (TP)	False Positive (FP)	True Negative (TN)	False Negative (FN)
1	16,977	1,809	193,128	12,463
2	18,344	692	190,605	15,446
3	16,847	1,284	191,550	16,046
4	13,723	386	196,837	16,631
5	14,690	676	196,105	16,222
6	15,188	742	194,641	16,928
7	14,359	1,139	196,384	15,793
8	13,811	1,471	195,388	14,578
9	13,003	914	200,005	13,738
10	12,546	806	199,370	14,610
11	14,728	1,248	197,027	14,811
12	15,414	1,383	195,280	13,076
13	14,424	513	197,732	17,835
14	16,518	2,734	196,433	10,159

15	12,821	2,275	201,505	10,793
16	15,130	1,235	196,668	14,661
17	14,783	1,863	196,169	13,069
18	15,184	2,531	198,937	10,960
19	16,658	953	199,064	10,713
20	13,386	1,839	201,419	10,879

Table 4.4.3: Fraction value of TP, FP, TN and FN

Image sequence	Fraction of True Positive (TP)	Fraction of False Positive (FP)	Fraction of True Negative (TN)	Fraction of False Negative (FN)
1	0.9307	0.0963	0.9394	0.0606
2	0.9636	0.0364	0.9250	0.0750
3	0.9292	0.0708	0.9227	0.0773
4	0.9726	0.0274	0.9221	0.0779
5	0.9560	0.0440	0.9236	0.0764
6	0.9534	0.0466	0.9200	0.0800
7	0.9265	0.0735	0.9256	0.0744
8	0.9037	0.0963	0.9306	0.0694
9	0.9343	0.0657	0.9357	0.0643
10	0.9396	0.0604	0.9317	0.0683
11	0.9219	0.0781	0.9301	0.0699
12	0.9177	0.0823	0.9380	0.0620
13	0.9657	0.0343	0.9161	0.0839
14	0.8580	0.1420	0.9508	0.0492
15	0.8493	0.1507	0.9492	0.0508
16	0.9245	0.0755	0.9306	0.0694

17	0.8881	0.1119	0.9375	0.0625
18	0.8571	0.1429	0.9478	0.0522
19	0.9459	0.0541	0.9489	0.0511
20	0.8792	0.1208	0.9488	0.0512

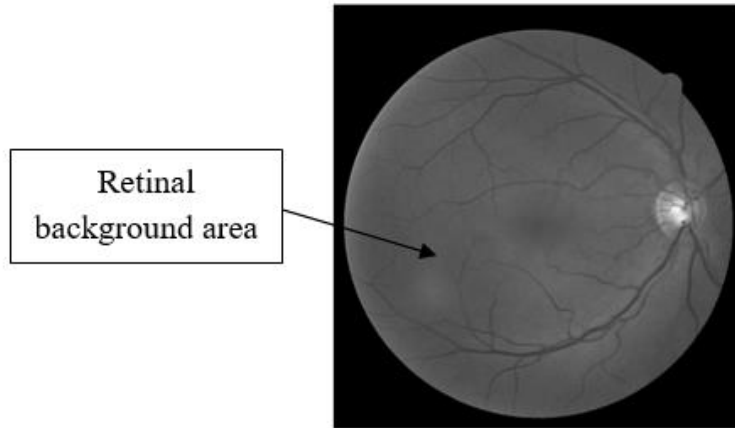


Figure 4.4.1: Retinal Background Area

The value of TN was large as it covered the whole retinal background (FOV) area to detect non-blood vessel pixel. As the blood vessel pixels only take up a small portion in the retinal background area (the rest are non-blood vessel pixels), this made the value of the TN much larger as compared to the value of TP, FP and FN. From the value of TP, FP, TN and FN, FP has the smallest value while TN has the largest value and value of TP and FN are close to each other. After obtaining the value for TP, FP, TN and FN, performance calculation could be done. Performance calculation was based on the parameters utilized in Marín et al. [27] which were:

$$Sensitivity (SE) = \frac{TP}{(TP + FN)}$$

$$Specificity (SP) = \frac{TN}{(TN + FP)} \quad (3)$$

$$Accuracy (ACC) = \frac{TP + TN}{FOV}$$

Table 4.4.3 shows the results evaluation of the proposed vessel extraction algorithm with the manually extracted vessel results (gold standard) from DRIVE database. Field of view (FOV) area for every fundus image is obtained using mask image (i.e. pixel =1) provided for each respective fundus images in DRIVE database and values of FOV were provided in Table 4.4.4. SE and SP values should be close to 1 for superior results on vessel extraction. However, FOV values for all fundus images were set to 229,052 to normalized the results of the proposed vessel extraction algorithm. The proposed vessel extraction algorithm has an average 51.86% sensitivity rate and specificity rate of 99.33% as well as 93.26% accuracy rate respectively, in DRIVE database.

The value of SE is quite low as the difference between both TP and FN values are small (large FN value). As shown in the formula, SE and ACC are dependent on TN value, thus the value of SE and ACC were high because the value of TN (TN pixels are non-blood vessel region which is the majority region of the image) is much larger as compared to FP and FN values. The value of FN is high and improvement could be made by minimizing the FN value for better performance. To have higher SE, SP and ACC, the value of TP and TN much be much larger than the value of FP and FN. Comparisons were done between the acquired results with other algorithms [27-33] and summarized in Table 4.4.4.

Table 4.4.4: Results Evaluation with DRIVE Database

IMAGE SEQUENCE	SENSITIVITY	SPECIFICITY	ACCURACY	FOV
1	0.5767	0.9907	0.9173	224,377
2	0.5429	0.9964	0.9122	225,087
3	0.5122	0.9933	0.9098	225,727
4	0.4521	0.9980	0.9193	227,577
5	0.4752	0.9966	0.9203	227,693
6	0.4729	0.9962	0.9161	227,499
7	0.4762	0.9942	0.9201	227,675

8	0.4865	0.9925	0.9133	225,248
9	0.4863	0.9955	0.9300	227,660
10	0.4620	0.9960	0.9252	227,332
11	0.4986	0.9937	0.9245	227,814
12	0.5410	0.9931	0.9306	227,605
13	0.4471	0.9974	0.9131	227,500
14	0.6192	0.9863	0.9297	225,854
15	0.5429	0.9888	0.9357	227,394
16	0.5079	0.9938	0.9247	227,694
17	0.5308	0.9906	0.9210	225,884
18	0.5808	0.9874	0.9348	227,612
19	0.6086	0.9952	0.9418	227,388
20	0.5517	0.9910	0.9378	227,523

Table 4.4.5: Performance Calculation Comparisons

<i>Algorithm</i>	Sensitivity (%)	Specificity (%)	Accuracy (%)
<i>Proposed algorithm</i>	51.86	99.33	93.26
<i>Marín et al. [27] (2011)</i>	70.67	98.01	94.52
<i>Raja et al. [28] (2015)</i>	93.99	98.37	98.08
<i>Fraz et al. [29] (2012)</i>	74.06	98.07	94.8
<i>Xiao et al. [30] (2013)</i>	75.13	97.92	95.29
<i>Budai et al. [31] (2013)</i>	64.40	98.70	95.72
<i>Manoj et al. [32] (2013)</i>	94.29	98.75	96.23
<i>Bansal and Dutta [33] (2006)</i>	86.53	98.33	97.28

4.5 Future Work

As mentioned previously there are 2 more stages that were not fully completed in this research i.e. artery/vein classification and AVR computation and should be the future work for this research i.e. to make an algorithm that automated the artery/vein classification and AVR estimation. A brief explanation was provided previously on the method that could be implemented to classify vessel into artery and vein. Once the classification was done, the final step could be executed i.e. computation of AVR which could be used to detect the presence and severity of hypertensive retinopathy. Diagnosing the presence of hypertensive retinopathy in patients through fundus image is a crucial step to pave the way for a more sophisticated stroke prediction model. Although with the rapid advancement in technology, there is still no simple and robust algorithm to foretell the assault from stroke. Even with the mentioned CHADS₂ score, there are still many required parameters for stroke prediction. This research was done with the hope on creating an ideal model for stroke prediction where hypertensive retinopathy was the only parameter required for the model. Besides that, there are various room for improvements in the field of retinal image processing as the current technology is still not on par with manual labelling.

CHAPTER 5

CONCLUSION AND RECOMMENDATION

Early diagnosis of signs related to hypertensive retinopathy is crucial in preventing the condition from worsening to a stage where the damage caused is permanent and irreversible. Thus, a simple method was proposed to identify and extract vessels from fundus image. Arterio-Venous Ratio (AVR) could be obtained through venular caliber measurement from the fundus image and should be applied to assess the severity of the hypertensive retinopathy. Model for assessing the hypertensive retinopathy could be completed once the final two stages i.e. artery/vein classification and AVR computation were completed.

There is always room for improvement for the algorithm proposed in this paper. Improvement can also be made to the vessels to make it more apparent and at the same time eliminating noise present. Besides that, preprocessing stage of the fundus image could be further improved for clearer retinal signs by filtering background noise using multiple filters such as Gaussian filter, mean filter and median filter to remove different types of noise i.e. salt and pepper noise, grain noise and Gaussian noise.

The author hopes that this paper would provide some insights and motivation to other researchers in the field of image processing. This paper was written with the intention to spark students' interest in imaging and hope that the future work on stroke prediction will be taken by young promising researcher. The also author hopes that this paper would be beneficial to any researcher that is working on retinal image processing and analysis.

REFERENCES

- [1] Dashtbozorg, B., Mendonca, A. M., & Campilho, A. (2013). An automatic graph-based approach for artery/vein classification in retinal images. *IEEE Transactions on Image Processing*, 1.
- [2] Henderson AD, Bruce BB, Newman NJ, et al. Hypertension-related eye abnormalities and the risk of stroke. *Reviews in neurological diseases*. 2011;8:1–9.
- [3] K Narasimhan, VC Neha, K Vijayarekha. Hypertensive retinopathy diagnosis from fundus images by estimation of AVR. *Procedia engineering* 12/2012; 38:980-993. DOI: 10.1016/j.proeng.2012.06.124
- [4] M. Al-Rawi, M. Qutaishat, and M. Arrar, “An improved matched filter for blood vessel detection of digital retinal images,” *Comput. Biol. Med.*, vol. 37, pp. 262–267, 2007.
- [5] M. Baker, P. Hand, J. Wang, and T. Wong, “Retinal signs and stroke,” *Stroke*, vol. 39, no. 4, pp. 1371–1379, 2008.
- [6] M. Niemeijer, J. Staal, B. Ginneken, M. Loog, and M. Abramoff. (2004).DRIVE: Digital Retinal Images for Vessel Extraction [Online]. Available: <http://www.isi.uu.nl/Research/Databases/DRIVE>
- [7] Roy PK, Nguyen UT, Bhuiyan A, Ramamohanarao K. An effective automated system for grading severity of retinal arteriovenous nicking in colour retinal images. *Conf Proc IEEE Eng Med Biol Soc* 2014; 2014:6324–6327.
- [8] T. Wong, R. Klein, B. Klein, J. Tielsch, L. Hubbard, and F. Nieto, “Retinal microvascular abnormalities and their relationship with hypertension, cardiovascular disease, and mortality,” *Survey of ophthalmology*, vol. 46, no. 1, pp. 59–80, 2001.
- [9] U. T. V. Nguyen, A. Bhuiyan, L. A. F. Park, and K. Ramamohanarao, “An effective retinal blood vessel segmentation method using multi-scale line detection,” *Pattern Recognit.*, vol. 46, no. 3, pp. 703–715, 2012.
- [10] U. T. V. Nguyen, A. Bhuiyan, L. A. F. Park, R. Kawasaki, T. Y. Wong, J. J. Wang, P. Mitchell, and K. Ramamohanarao, “Automated quantification of retinal arteriovenous nicking from colour fundus images,” in *Proc. IEEE 35th Annu. Int. Conf. Eng. Med. Biol. Soc.*, 2013, pp. 5865–5868.
- [11] (2010). VICAVR: VARPA Images for the Computation of the Arterio/ Venular Ratio [Online]. Available: <http://www.varpa.es/vicavr.html>
- [12] Morillas P, Pallarés V, Fácila L, Llisterri JL, et al. The CHADS2 score to predict stroke risk in the absence of atrial fibrillation in hypertensive patients aged 65 years or older. *Rev Esp Cardiol (Engl Ed)*. 2014; 1-7.
- [13] O.Brinchmann-Hansen and H.Heier, “Theoretical relationships between light streak characteristics optical properties of retinal vessels,” *Acta Ophthalmologica, Suppl.*, vol. 179, pp. 33-37, 1986.
- [14] M. Kalavani¹, M. S. Jeyalakshmi², Aparna.V³; Extraction Of Retinal Blood Vessels Using Curvelet Transform And Kirsch’s Templates ; *International Journal of Emerging Technology and Advanced Engineering Website: www.ijetae.com (ISSN 2250-2459, Volume 2, Issue 11, November 2012).*

- [15] Coye, Tyler (2015). A Novel Retinal Blood Vessel Segmentation Algorithm for Fundus Images (<http://www.mathworks.com/matlabcentral/fileexchange/50839>), MATLAB Central File Exchange.[Jan 19], [2017].
- [16] Manjiri B. Patwari, Ramesh R. Manza, Yogesh M. Rajput, Deepali D. Rathod, Manoj Saswade, Neha Deshpande, "Classification and Calculation of Retinal Blood vessels Parameters", IEEE's INTERNATIONAL CONFERENCES FOR CONVERGENCE OF TECHNOLOGY, Pune,India.
- [17] Patwari Manjiri, Manza Ramesh, Rajput Yogesh, Saswade Manoj, Deshpande Neha, "Automated Localization of Optic Disk, Detection of Microaneurysms and Extraction of Blood Vessels to Bypass Angiography", Springer, Advances in Intelligent Systems and Computing. ISBN: 978-3-319-11933-5, DOI: 10.1007/978-3-319-11933-5_65. 2014.
- [18] Manjiri B. Patwari, Ramesh R. Manza, Yogesh M. Rajput, Manoj Saswade, Neha K. Deshpande, "Detection and Counting the Microaneurysms using Image Processing Techniques" International Journal of Applied Information Systems (IJ AIS) – 6(5):11-17, November 2013. Published by Foundation of Computer Science, New York, USA., ISSN : 2249-0868, Vol. 6 Number 5, October - 2013, IF 1.187.
- [19] S. G. Vázquez, B. Cancela, N. Barreira, M. G. Penedo, M. Rodríguez-Blanco, M. Pena, G. Coll de Tuero, M. A. Barceló, M. Saez, "Improving retinal artery and vein classification by means of a minimal path approach", Machine Vision and Applications, 24(5), 919-930, 2013.
- [20] Yogesh M. Rajput, Ramesh R. Manza, Manjiri B. Patwari, Neha Deshpande, "Retinal Blood Vessels Extraction Using 2D Median Filter", Third National Conference on Advances in Computing(NCAC-2013), 5th to 6th March 2013, School of Computer Sciences, North Maharashtra University, Jalgaon-425001 (MS) India.
- [21] Rani, Anju. Detection of Hypertensive Retinopathy through Color Fundus Images. Diss. Thapar University, Patiala, 1956.
- [22] Uyen T. V. Nguyen, Alauddin Bhuiyan, Laurence A.F. Park, Ryo Kawasaki, Tien Y Wong, Jie Jin Wang, Paul Mitchell and Kotagiri Ramamohanarao, "An Automated Method for Retinal Arteriovenous Nicking Quantification From Color Fundus Images", IEEE Transactions on Biomedical Engineering, vol. 60, number.11, pp. 3194–3203, 2013.
- [23] G.C. Manikis, V. Sakkalis, X. Zabulis, P. Karamaounas, A.Triantafyllou, S. Douma, C. Zamboulis, K. Marias, *An Image Analysis Framework for the Early Assessment of Hypertensive Retinopathy Signs*. Proceedings of the 3rd International Conference on E-Health and Bioengineering – EHB 2011,24th-26thNovember, 2011, Iași, Romania.
- [24] N.M. Keith, H.P. Wagener, N.W. Barker (1939), *Some different types of essential hypertension: their course and prognosis*. Am J Med Sci, 197, 332–43.
- [25] J.J. Staal, M.D. Abramoff, M. Niemeijer, M.A. Viergever, B. van Ginneken, "Ridge based vessel segmentation in color images of the retina", IEEE Transactions on Medical Imaging, 2004, vol. 23, pp. 501-509.
- [26] Hough PVC. Method and means for recognizing complex patterns. US Patent 3, 069, 654, December 18, 1962.

- [27] D. Marín, A. Aquino, M. E. Gegúndez-Arias, and J. M. Bravo, “A new supervised method for blood vessel segmentation in retinal images by using gray-level and moment invariants-based features,” *IEEE Transactions on Medical Imaging*, vol. 30, no. 1, pp. 146–158, 2011.
- [28] Raja DS, Vasuki S. “Automatic detection of blood vessels in retinal images for diabetic retinopathy diagnosis”. *Comput Math Methods Med.* 2015; 2015: 419279.
- [29] M. M. Fraz, P. Remagnino, A. Hoppe et al., “An ensemble classification-based approach applied to retinal blood vessel segmentation,” *IEEE Transactions on Biomedical Engineering*, vol. 59, no. 9, pp. 2538–2548, 2012.
- [30] Z. Xiao, M. Adel, and S. Bourennane, “Bayesian method with spatial constraint for retinal vessel segmentation,” *Computational and Mathematical Methods in Medicine*, vol. 2013, Article ID 401413, 9 pages, 2013.
- [31] A. Budai, R. Bock, A. Maier, J. Hornegger, and G. Michelson, “Robust vessel segmentation in fundus images,” *International Journal of Biomedical Imaging*, vol. 2013, Article ID 154860, 11 pages, 2013.
- [32] S. Manoj, Muralidharan, and P. M. Sandeep, “Neural network based classifier for retinal blood vessel segmentation,” *International Journal of Recent Trends in Electrical & Electronics Engineering*, vol. 3, no. 1, pp. 44–53, 2013.
- [33] N. Bansal and M. Dutta, “Retina vessels detection algorithm for biomedical symptoms diagnosis,” *International Journal of Computer Applications*, vol. 71, no. 20, pp. 41–46, 2013

APPENDIX

Code (Red, Green and Blue Channels extraction)

```
% Getting input image
In = imread('C:\Users\User\Documents\Degree\Final Final\FYP 1\Sample\VICAVR\images\original\Image1.jpg');
In = imresize(In,[500 700]); % Resizing image

redc = In(:,:,1); % Storing Red Plane
greenc = In(:,:,2); % Storing Green Plane
bluec = In(:,:,3); % Storing Blue Plane
subplot(2,2,1), imshow(In), title('(a) Original Image');
subplot(2,2,2), imshow(redc), title('(b) Red Channel');
subplot(2,2,3), imshow(greenc), title('(c) Green Channel');
subplot(2,2,4), imshow(bluec), title('(d) Blue Channel');
```

Code (Creating Fundus Mask)

```
In = imread('C:\Users\User\Documents\Degree\Final Final\FYP 1\Sample\VICAVR\images\original\Image1.jpg');
In = imresize(In,[500 700]);

redc = In(:,:,1); % Storing Red Plane
mask = im2bw(redc,graythresh(redc)); % Finding the threshold
mask = bwareaopen(mask,100); % Binary morphological opening
mask = imfill(mask,'holes');
figure, imshow(mask);

%apply mask to eliminate background noise
greenc(~mask) = 0;
```

Code (Extracting vessel)

```
clear all;
close all;
clc;
In = imread('C:\Users\User\Documents\Degree\Final Final\FYP 1\Sample\VICAVR\images\original\Image1.jpg');

redc = In(:,:,1); % Extract Red Channel
greenc = In(:,:,2); % Extract Green Channel
bluec = In(:,:,3); % Extract Blue Channel

subplot(2,2,1), imshow(In), title('(a) Original Image');
subplot(2,2,2), imshow(redc), title('(b) Red Channel');
subplot(2,2,3), imshow(greenc), title('(c) Green Channel');
subplot(2,2,4), imshow(bluec), title('(d) Blue Channel');
figure, imshow(In);

subplot(2,2,3), imhist(redc), title('(b) Red Channel');
subplot(2,2,[1,2]), imhist(greenc), title('(c) Green Channel');
subplot(2,2,4), imhist(bluec), title('(d) Blue Channel');
%lab = rgb2lab(I);
% figure, imhist(redc);
% figure, imhist(greenc);
% h(1) = imshow(greenc);

maxgc = max(max(greenc))
[row,column] = find(greenc >= maxgc*0.99)
meangc = mean(greenc);
```

```

%z = zscore(greenc);

% b = imregionalmax(greenc);
% imshow (b);

% c = rgb2hsl(In);
% c = hsl(:,:,3);
% imshow (c);

% a = 255*0.99;
% idx = kmeans(a);
% imshow (idx);

% Creating fundus mask
mask = im2bw(redec,graythresh(redec));
mask = bwareaopen(mask,100);
mask = imfill(mask,'holes');
figure, imshow(mask);

%apply mask to eliminate background noise
greenc(~mask) = 0;
figure, imshow(greenc);
[centers, radii] = imfindcircles(greenc, [245 255], 'Sensitivity', 0.99);
viscircles(centers,radii);
% set(h(1),'cdata',greenc);
% vesselmask = edge(greenc,'canny',0.10,1);
% vs = imgca;
% figure, imshow(vesselmask);
%
% vesselmask(~imerode(mask,strel('disk',6)))=0;
%
% % dilation
% vesselmask=imdilate(vesselmask,strel('disk',5));
% figure, imshow(vesselmask);
% vesselmask = bwmorph(vesselmask,'dilate');
% vesselmask=bwmorph(vesselmask,'skel',Inf);
% vesselmask = bwmorph(vesselmask,'bridge');
% vesselmask=bwmorph(vesselmask,'skel',Inf);
% vesselmask=bwmorph(vesselmask,'spur',5);
% %
% vesselmask=bwmorph(vesselmask,'skel',Inf);
% figure, imshow(vesselmask);
% branchPoints=bwmorph(vesselmask,'branch',1);
% branchPoints=imdilate(branchPoints,strel('disk',2));
% figure, imshow(branchPoints)
% bp=imgca;
% % %
% vesselmask = bwmorph(vesselmask,'dilate');
% vesselmask=vesselmask & ~ branchPoints;
% figure, imshow(vesselmask)

ginv = imcomplement (greenc);           % Complement the Green Channel (Vessel are lighter than background)
ginv = medfilt2(ginv);
adahist = adapthisteq(ginv);           % Adaptive Histogram Equalization

figure, subplot(1,2,1), imshow(ginv), title ('(a) Complementary Fundus Image');
subplot(1,2,2), imshow(adahist), title ('(b) CLAHE Transformation');

adahist = medfilt2(adahist);

tophat = imtophat(adahist,strel('disk',8));

%tophat1=tophat;
tophat(~mask)=0;
bothat = imbothat(adahist, strel('disk',8));
figure, imshow(tophat);
figure, imshow(bothat);
a = imsubtract(tophat,bothat);
figure, imshow(a), title('a');

```

```

% % Detection of microaneurysms
% adjustIm = imadjust(adahist,[],[],3);
% comp = imcomplement(adjustIm);
% J = imadjust(comp,[],[],4);
% J = imcomplement(J);
% J = imadjust(J,[],[],4);
% K=fspecial('disk',5);
% L=imfilter(J,K,'replicate');
% L = im2bw(L,0.4);
% M = bwmorph(L,'tophat');
% figure, imshow (M);
% % M = im2bw(M);
% wname = 'sym4';
% [CA,CH,CV,CD] = dwt2(M,wname,'mode','per');
% figure,imshow(CA);
%
% b = bwboundaries(CA);
% % Im = imresize(In,[303 350]);
% %figure, imshow(Im);
% hold on
% for area_bloodvessels = 1:numel(b)
%     plot(b{area_bloodvessels}(:,2), b{area_bloodvessels}(:,1), 'b', 'Linewidth', 1)
% end

se = strel('ball',8,8);           % Structuring Element
gopen = imopen(a,se);           % Morphological Open (thickening vessel)
figure, imshow(gopen);
godisk = a - gopen;             % Remove bright lesions in Optic Disk
figure, subplot(1,2,1), imshow(gopen), title('(a)');
subplot(1,2,2), imshow(godisk), title('(b)');
medfilt = medfilt2(godisk);     % 2D Median Filter
background = imopen(medfilt,strel('disk',15));% imopen function
I2 = medfilt - background;     % Remove Background
I3 = imadjust(I2);             % Image Adjustment
mean1 = mean(I3);
figure, imshow(mean1);
figure, subplot(2,2,1), imshow(medfilt), title('(a)');
subplot(2,2,2), imshow(background), title('(b)');
subplot(2,2,[3,4]), imshow(I3), title('(c)');
figure,imshow(I3);

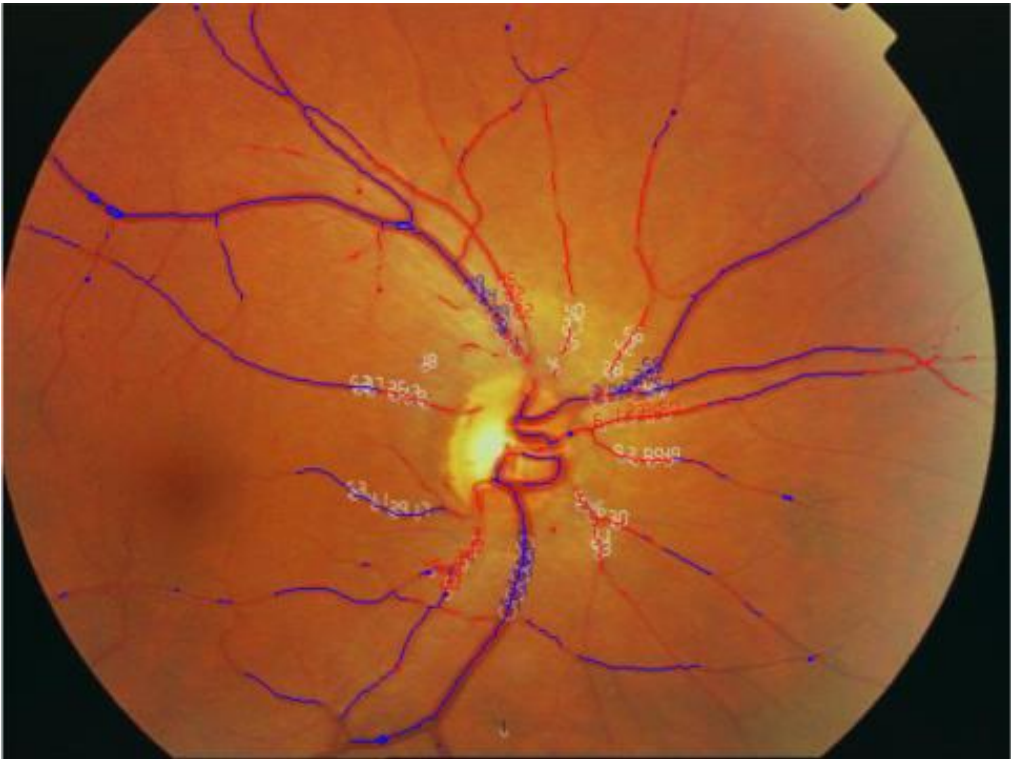
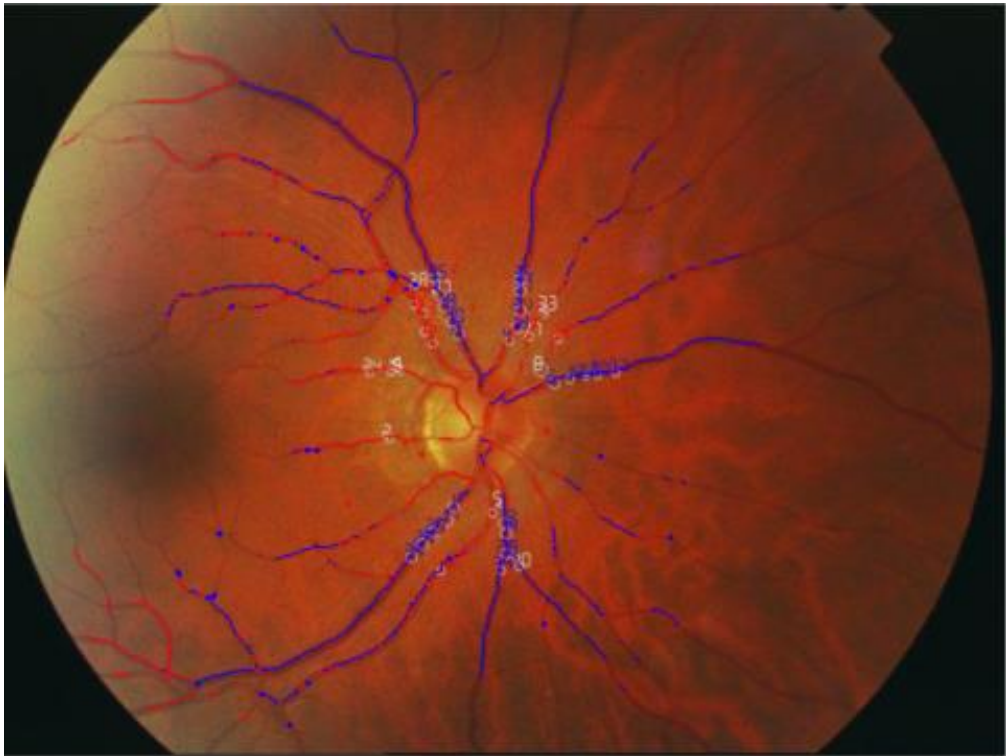
%OD = detectSURFFeatures(I3);
%figure,imshow(I3),title('I3'); hold on;
%plot(OD.selectStrongest(10));
%h = imellipse
% B1 = bitget(I3,7); figure, imshow(logical(B1));
% B2 = bitget(I3,8); figure, imshow(logical(B2));
% figure, imshow(logical(B1+B2));
level = graythresh(I3)         % Gray Threshold
bw = im2bw(I3,level);         % Binarization
bw = bwareaopen(bw, 30);      % Morphological Open

edtIM = bwdist(~bw);
figure, imshow(edtIM,[]), title('edt');
drawnow;
skelIM = bwmorph(bw,'skel', inf);
%diameterImage
%save('segmented_vessel.mat', 'bw');
skelIM = bwmorph(skelIM,'spur',5);
[labeledImage, numLines] = bwlabel(skelIM);
figure, imshow(skelIM, []);
branchpoints = bwmorph(skelIM,'branch',1);
branchpoints = imdilate(branchpoints,strel('disk',2));
figure,imshow(bw);

figure, imshow(skelIM);
figure, imshow(branchpoints);
% [r,c] = find(skelIM,409,337)
meanRadius = mean(edtIM(skelIM));

```

Overlaying of Classified Vessel



Code for Artery/Vein Classification

```
clear all;
close all;
clc;
In = imread('C:\Users\User\Documents\Degree\Final Final\FYP 1\Sample\VICAVR\images\original\Image36.jpg');
yo = imread('C:\Users\User\Documents\Degree\Final Final\FYP 1\Sample\VICAVR\images\expert1\Image36.jpeg');

redc = In(:,:,1);           % Extract Red Channel
greenc = In(:,:,2);        % Extract Green Channel
bluec = In(:,:,3);        % Extract Blue Channel
%greenc = imopen(greenc,(strel('disk',1)));
subplot(2,2,1), imshow(In), title('(a) Original Image');
subplot(2,2,2), imshow(redc), title('(b) Red Channel');
subplot(2,2,3), imshow(greenc), title('(c) Green Channel');
subplot(2,2,4), imshow(bluec), title('(d) Blue Channel');
figure, imshow(In);

%subplot(2,2,1), imhist(In), title('(a) Original Image');
%subplot(2,2,3), imhist(redc), title('(b) Red Channel');
%subplot(2,2,[1,2]), imhist(greenc), title('(c) Green Channel');
%subplot(2,2,4), imhist(bluec), title('(d) Blue Channel');

maxgc = max(max(greenc))
[row,column] = find(greenc >= maxgc*0.99)
meangc = mean(greenc);

% Creating fundus mask
mask = im2bw(redc,graythresh(redc));
mask = bwareaopen(mask,100);
mask = imfill(mask,'holes');
figure, imshow(mask);

%apply mask to eliminate background noise
greenc(~mask) = 0;
ginv = imcomplement (greenc);           % Complement the Green Channel (Vessel are lighter than background)
ginv = medfilt2(ginv);
adahist = adapthisteq(ginv);           % Adaptive Histogram Equalization

adahist = medfilt2(adahist);

tophat = imtophat(adahist,strel('disk',8));
tophat(~mask)=0;
bothat = imbothat(adahist, strel('disk',8));
a = imsubtract(tophat,bothat);
test= a-greenc;
test = imcomplement(test);

%
se = strel('ball',8,8);           % Structuring Element
gopen = imopen(a,se);           % Morphological Open (thickening vessel)
figure, imshow(gopen);
godisk = a - gopen;           % Remove bright lesions in Optic Disk
medfilt = medfilt2(godisk);     % 2D Median Filter
background = imopen(medfilt,strel('disk',15));% imopen function
I2 = medfilt - background;     % Remove Background
I3 = imadjust(I2);           % Image Adjustment
meanI = mean(I3);
level = graythresh(I3)         % Gray Threshold
bw = im2bw(I3,level);         % Binarization
bw = bwareaopen(bw, 30);      % Morphological Open

edtIM = bwdist(~bw);
figure, imshow(edtIM,[]), title('edt');
drawnow;
skelIM = bwmorph(bw,'skel', inf);
skelIM = bwmorph(skelIM,'spur',5);
[labeledImage, numLines] = bwlabel(skelIM);
figure, imshow(skelIM, []);
```

```

branchpoints = bwmorph(skelIM,'branch',1);
branchpoints = imdilate(branchpoints,strel('disk',2));
figure,imshow(bw), title('bw');

sample=edtIM(skelIM);
%%
bv = im2uint8(bw)./255;
skelIm = im2uint8(skelIM)./255;
greenc=medfilt2(greenc);
redc=medfilt2(redc);
bluec=medfilt2(bluec);
vgreenint=greenc.*bv;
vredint=redc.*bv;
vblueint=bluec.*bv;
maxr=max(max(vredint));
maxg=max(max(vgreenint));
maxb=max(max(vblueint));
minr=min(min(vredint(vredint>0)));
ming=min(min(vgreenint(vgreenint>0)));
minb=min(min(vblueint(vblueint>0)));
numr=0;
numg=0;
numb=0;
numh=0;
nums=0;
numv=0;
greenint=greenc.*skelIm;
redint=redc.*skelIm;
blueint=bluec.*skelIm;
% figure, imhist(redint,1000000);
% figure, imhist(greenint,1000000);
% figure, imhist(blueint,1000000);
% figure, imtool(redint), title('redint');
% figure, imtool(blueint), title('blueint');
% figure, imshow(greenint), title('greenint');
% overlay=imoverlay(In, skelIm)
bv2 = im2double(bw)
skelIm2 = im2double(skelIm)
hsv_value = rgb2hsv(In);
figure, imshow(hsv_value), title('hsv');
h = hsv_value(:,:,1);
s = hsv_value(:,:,2);
v = hsv_value(:,:,3);
i = sum((double(In)/255),3)/3;
h_intv=h.*bv2;
s_intv=s.*bv2;
v_intv=v.*bv2;
i_intv=i.*bv2;
h_int=h.*skelIm2;
s_int=s.*skelIm2;
v_int=v.*skelIm2;
i_int=i.*skelIm2;
maxh=max(max(h_intv));
maxs=max(max(s_intv));
maxi=max(max(i_intv));
minh=min(min(h_intv(h_intv>0)));
mins=min(min(s_intv(s_intv>0)));
mini=min(min(i_intv(i_intv>0)));
numg1=0;
% figure, imshow(skelIm2), title('h_int');

% vmeang=sum(sum(vgreenint))/numg % mean of green channel
% vmeanr=sum(sum(vredint))/numr % mean of red channel
% vmeanb=sum(sum(vblueint))/numb % mean of blue channel
% vmeanh=sum(sum(h_intv))/numh % mean of hue channel
% vmeans=sum(sum(s_intv))/nums % mean of saturation channel
% vmeanv=sum(sum(v_intv))/numv % mean of value channel
vmeang=mean2(vgreenint(vgreenint>0))
vmeanr=mean2(vredint(vredint>0))
vmeanb=mean2(vblueint(vblueint>0))

```

```

vmeanh=mean2(h_intv(h_intv>0))
vmeans=mean2(s_intv(s_intv>0))
vmeani=mean2(i_intv(i_intv>0))
stdg = im2double(vgreenint);
stdr = im2double(vredint);
stdb = im2double(vblueint);
stdh = im2double(h_intv);
stds = im2double(s_intv);
stdi = im2double(i_intv);
vstdg = std2(stdg(stdg>0))
vstdr = std2(stdr(stdr>0))
vstdb = std2(stdb(stdb>0))
vstdh = std2(stdh(stdh>0))
vstds = std2(stds(stds>0))
vstdi = std2(stdi(stdi>0))
figure, imshow (vredint), title('redint');
mean_g = mean(greenint);
mean_r = mean(redint);
mean_b = mean(blueint);
for a=1:768
    for b=1:576
        if(greenint(b,a)>vmeang)
            red(b,a) = greenint(b,a);
        else
            blue(b,a) = greenint(b,a);
        end
        if(vgreenint(b,a)>0)
            numg=numg+1;
        end
        if(vredint(b,a)>181)
            numg1=numg1+1;
        end
        if(vredint(b,a)>0)
            numr=numr+1;
        end
        if(vblueint(b,a)>0)
            numb=numb+1;
        end
        if(h_intv(b,a)>0)
            numh=numh+1;
        end
        if(s_intv(b,a)>0)
            nums=nums+1;
        end
        if(v_intv(b,a)>0)
            numv=numv+1;
        end
    end
end
wname = 'sym4';
[CA,CH,CV,CD] = dwt2(red,wname,'mode','per');
figure,imshow(CA),title('Approximate');
b = bwboundaries(red);

figure,imshow(yo)
hold on
for k = 1:numel(b)
    plot(b{k}(:,2), b{k}(:,1), 'r', 'Linewidth', 1)
end
c = bwboundaries(blue);
for k = 1:numel(c)
    plot(c{k}(:,2), c{k}(:,1), 'b', 'Linewidth', 1)
end
figure, imshow(red), title('red');
meanRadius = mean(edtIM(skelIM));

%RGB vein 36
veing(1)=sum(impixel(greenc,330,209))/3;
veinr(1)=sum(impixel(redec,330,209))/3;
veinb(1)=sum(impixel(bluec,330,209))/3;

```

```

veing(2)=sum(impixel(greenc,395,210))/3;
veinr(2)=sum(impixel(redc,395,210))/3;
veinb(2)=sum(impixel(bluec,395,210))/3;
veing(3)=sum(impixel(greenc,468,281))/3;
veinr(3)=sum(impixel(redc,468,281))/3;
veinb(3)=sum(impixel(bluec,468,281))/3;
vein_green = veing
vein_red = veinr
vein_blue = veinb
mean_veinr=mean(veinr)
mean_veing=mean(veing)
mean_veinb=mean(veinb)
std_veinb=std(veinb)
std_veinr=std(veinr)
std_veing=std(veing)
std_veinb=std(veinb)
% %37
% veing(1)=sum(impixel(greenc,397,410))/3;
% veinr(1)=sum(impixel(redc,397,410))/3;
% veinb(1)=sum(impixel(bluec,397,410))/3;
% veing(2)=sum(impixel(greenc,485,288))/3;
% veinr(2)=sum(impixel(redc,485,288))/3;
% veinb(2)=sum(impixel(bluec,485,288))/3;
% veing(3)=sum(impixel(greenc,357,217))/3;
% veinr(3)=sum(impixel(redc,357,217))/3;
% veinb(3)=sum(impixel(bluec,357,217))/3;
% vein_green = veing
% vein_red = veinr
% vein_blue = veinb
% mean_veinr=mean(veinr)
% mean_veing=mean(veing)
% mean_veinb=mean(veinb)
% std_veinb=std(veinb)
% std_veinr=std(veinr)
% std_veing=std(veing)
% std_veinb=std(veinb)

%RGB artery 36
arteryg(1)=sum(impixel(greenc,424,255))/3;
arteryr(1)=sum(impixel(redc,424,255))/3;
arteryb(1)=sum(impixel(bluec,424,255))/3;
arteryg(2)=sum(impixel(greenc,314,229))/3;
arteryr(2)=sum(impixel(redc,314,229))/3;
arteryb(2)=sum(impixel(bluec,314,229))/3;
arteryg(3)=sum(impixel(greenc,334,432))/3;
arteryr(3)=sum(impixel(redc,334,432))/3;
arteryb(3)=sum(impixel(bluec,334,432))/3;
artery_green = arteryg
artery_red = arteryr
artery_blue = arteryb
mean_arteryr=mean(arteryr)
mean_arteryg=mean(arteryg)
mean_arteryb=mean(arteryb)
%37
% arteryg(1)=sum(impixel(greenc,381,214))/3;
% arteryr(1)=sum(impixel(redc,381,214))/3;
% arteryb(1)=sum(impixel(bluec,381,214))/3;
% arteryg(2)=sum(impixel(greenc,455,321))/3;
% arteryr(2)=sum(impixel(redc,455,321))/3;
% arteryb(2)=sum(impixel(bluec,455,321))/3;
% arteryg(3)=sum(impixel(greenc,361,408))/3;
% arteryr(3)=sum(impixel(redc,361,408))/3;
% arteryb(3)=sum(impixel(bluec,361,408))/3;
% artery_green = arteryg
% artery_red = arteryr
% artery_blue = arteryb
% mean_arteryr=mean(arteryr)
% mean_arteryg=mean(arteryg)
% mean_arteryb=mean(arteryb)

```



```

%HSV vein 36
veinh(1)=sum(impixel(h,330,209))/3;
veins(1)=sum(impixel(s,330,209))/3;
veini(1)=sum(impixel(i,330,209))/3;
veinh(2)=sum(impixel(h,395,210))/3;
veins(2)=sum(impixel(s,395,210))/3;
veini(2)=sum(impixel(i,395,210))/3;
veinh(3)=sum(impixel(h,468,281))/3;
veins(3)=sum(impixel(s,468,281))/3;
veini(3)=sum(impixel(i,468,281))/3;
vein_hue = veinh
vein_sat = veins
vein_int = veini
mean_veinh=mean(veinh)
mean_veins=mean(veins)
mean_veini=mean(veini)

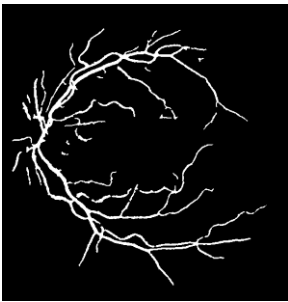
```

```

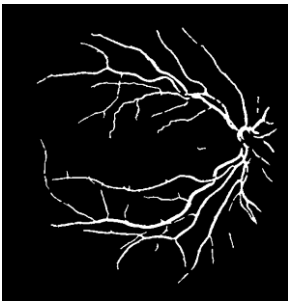
%HSV artery 36
arteryh(1)=sum(impixel(h,424,255))/3;
arterys(1)=sum(impixel(s,424,255))/3;
arteryi(1)=sum(impixel(i,424,255))/3;
arteryh(2)=sum(impixel(h,314,229))/3;
arterys(2)=sum(impixel(s,314,229))/3;
arteryi(2)=sum(impixel(i,314,229))/3;
arteryh(3)=sum(impixel(h,334,432))/3;
arterys(3)=sum(impixel(s,334,432))/3;
arteryi(3)=sum(impixel(i,334,432))/3;
artery_hue = arteryh
artery_sat = arterys
artery_int = arteryi
mean_arteryh=mean(arteryh)
mean_arterys=mean(arterys)
mean_arteryi=mean(arteryi)

```

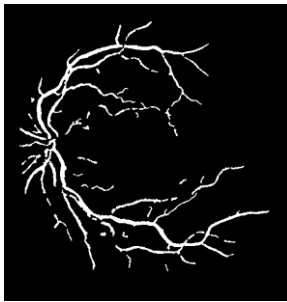
Extracted Vessel from DRIVE



(1)



(2)



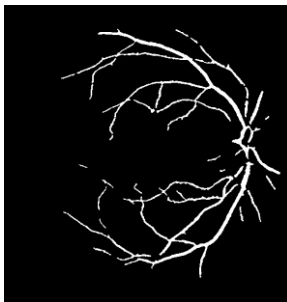
(3)



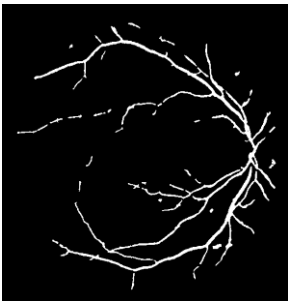
(4)



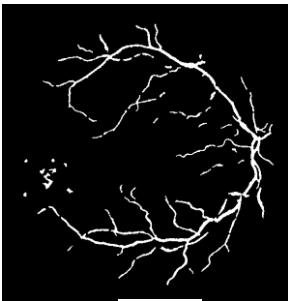
(5)



(6)



(7)



(8)



(9)



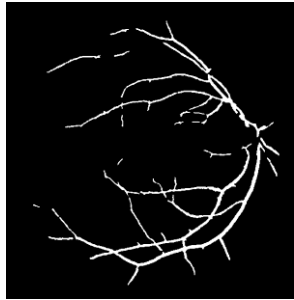
(10)



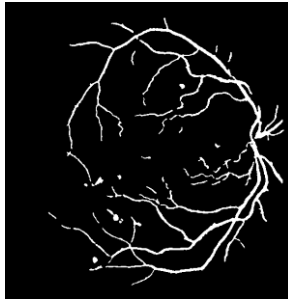
(11)



(12)



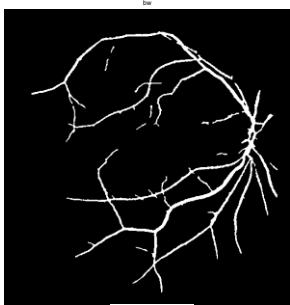
(13)



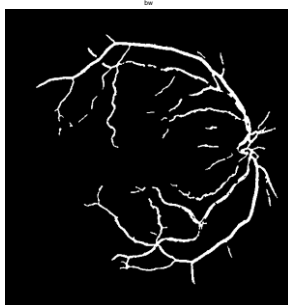
(14)



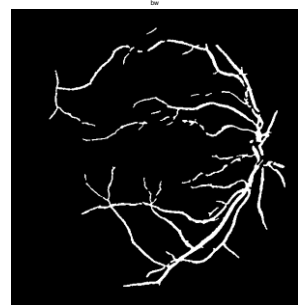
(15)



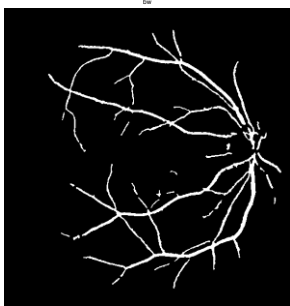
(16)



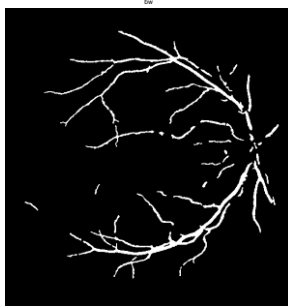
(17)



(18)



(19)



(20)

Code (Performance Analysis)

```
clear all;
close all;
clc;
In = imread('C:\Users\User\Documents\Degree\Final Final\FYP 1\Sample\DRIVE\test\images\20_test.tif');
Gold_std = imread('C:\Users\User\Documents\Degree\Final Final\FYP 1\Sample\DRIVE\test\1st_manual\20_manual1.gif');
fov = imread('C:\Users\User\Documents\Degree\Final Final\FYP 1\Sample\DRIVE\test\mask\20_test_mask.gif');
%In = imresize(In,[500 700]);

redc = In(:,:,1);           % Extract Red Channel
greenc = In(:,:,2);        % Extract Green Channel
bluec = In(:,:,3);        % Extract Blue Channel

subplot(2,2,1), imshow(In), title('(a) Original Image');
subplot(2,2,2), imshow(redc), title('(b) Red Channel');
subplot(2,2,3), imshow(greenc), title('(c) Green Channel');
subplot(2,2,4), imshow(bluec), title('(d) Blue Channel');
figure, imshow(In);

%subplot(2,2,1), imhist(In), title('(a) Original Image');
%subplot(2,2,3), imhist(redc), title('(b) Red Channel');
%subplot(2,2,[1,2]), imhist(greenc), title('(c) Green Channel');
%subplot(2,2,4), imhist(bluec), title('(d) Blue Channel');
%lab = rgb2lab(I);
% figure, imhist(redc);
% figure, imhist(greenc);
% h(1) = imshow(greenc);

maxgc = max(max(greenc))
[row,column] = find(greenc >= maxgc*0.99)
meangc = mean(greenc);

% Creating fundus mask
mask = im2bw(redc,graythresh(redc));
mask = bwareaopen(mask,100);
mask = imfill(mask,'holes');
figure, imshow(mask);

%apply mask to eliminate background noise
greenc(~mask) = 0;
figure, imshow(greenc);
ginv = imcomplement (greenc);           % Complement the Green Channel (Vessel are lighter than background)
ginv = medfilt2(ginv);
adahist = adapthisteq(ginv);           % Adaptive Histogram Equalization

figure, subplot(1,2,1), imshow(ginv), title('(a) Complementary Fundus Image');
subplot(1,2,2), imshow(adahist), title('(b) CLAHE Transformation');

adahist = medfilt2(adahist);

tophat = imtophat(adahist,strel('disk',8));

%tophat1=tophat;
tophat(~mask)=0;
bothat = imbothat(adahist, strel('disk',8));
figure, imshow(tophat);
figure, imshow(bothat);
a = imsubtract(tophat,bothat);
figure, imshow(a), title('a');
test= a-greenc;
test = imcomplement(test);
figure, imshow(test), title('test');
%
se = strel('ball',8,8);           % Structuring Element
gopen = imopen(a,se);           % Morphological Open (thickening vessel)
figure, imshow(gopen);
godisk = a - gopen;           % Remove bright lesions in Optic Disk
```

```

figure, subplot(1,2,1), imshow(gopen), title (('a'));
subplot(1,2,2), imshow(godisk), title (('b'));
%figure, imshow(gopen), title('gopen');
%figure, imshow(godisk), title('godisk');
%vesselMask(~imerode(greenc,strel('disk',6)));
%figure, imshow(vesselMask);
medfilt = medfilt2(godisk);           %2D Median Filter
background = imopen(medfilt,strel('disk',15));% imopen function
I2 = medfilt - background;           % Remove Background
I3 = imadjust(I2);                   % Image Adjustment
mean1 = mean(I3);
figure, imshow(mean1);
figure, subplot(2,2,1), imshow(medfilt), title (('a'));
subplot(2,2,2), imshow(background), title (('b'));
subplot(2,2,[3,4]), imshow(I3), title (('c'));
figure,imshow(I3);

level = graythresh(I3)               % Gray Threshold
bw = im2bw(I3,level);                % Binarization
bw = bwareaopen(bw, 30);              % Morphological Open

edtIM = bwdist(~bw);
figure, imshow(edtIM,[]), title ('edt');
drawnow;
skelIM = bwmorph(bw,'skel', inf);
skelIM = bwmorph(skelIM,'spur',5);
[labeledImage, numLines] = bwlabel(skelIM);
figure, imshow(skelIM, []);
branchpoints = bwmorph(skelIM,'branch',1);
branchpoints = imdilate(branchpoints,strel('disk',2));
figure,imshow(bw);

figure, imshow(skelIM);
figure, imshow(branchpoints);
meanRadius = mean(edtIM(skelIM));
%
Gold_std = logical(Gold_std);
figure, imshow(Gold_std), title('Gold Standard');
fov = logical(fov);
result = Gold_std & bw;
gold_zero=0;
gold_one=0;
bw_one=0;
bw_zero=0;
fn=0;
tn=0;
count=0;
fov_count=0;
fp=0;
zero=bw|Gold_std;
diff= bw - Gold_std;
tp = sum(sum(result));
for a=1:565
    for b=1:584
        if (diff(b,a)==1)
            fp=fp+1;
        end
        if (diff(b,a)==-1)
            fn=fn+1;
        end
        if (Gold_std(b,a)==0)
            gold_zero=gold_zero+1;
        end
        if (Gold_std(b,a)==1)
            gold_one=gold_one+1;
        end
        if (bw(b,a)==0)
            bw_zero=bw_zero+1;
        end
        if (bw(b,a)==1)

```

```
        bw_one=bw_one+1;
    end
    if (fov(b,a)==0)
        count=count+1;
    end
    if (fov(b,a)==1)
        fov_count=fov_count+1;
    end
    if (zero(b,a)==0)
        tn=tn+1;
    end
end
end
total = bw_one+bw_zero-count
tn = tn-count;
tpf = tp/bw_one
fpf = fp/bw_one
tnf = tn/(bw_zero-count)
fnf = fn/(bw_zero-count)
sensitivity = tp/(tp+fn)
specificity = tn/(tn+fp)
accuracy = (tp+tn)/229052
```